



# NIH Public Access

## Author Manuscript

*J Chem Neuroanat.* Author manuscript; available in PMC 2009 November 17.

Published in final edited form as:

*J Chem Neuroanat.* 2007 September ; 34(1-2): 1–21. doi:10.1016/j.jchemneu.2007.03.005.

## GABA Immunoreactivity in Auditory and Song Control Brain Areas of Zebra Finches

Raphael Pinaud<sup>1,2,\*</sup> and Claudio V. Mello<sup>1</sup>

<sup>1</sup> Laboratory of Auditory and Vocal Learning, Neurological Sciences Institute, Oregon Health and Sciences University, Portland, OR, USA

### Abstract

Inhibitory transmission is critical to sensory and motor processing and is believed to play a role in experience-dependent plasticity. The main inhibitory neurotransmitter in vertebrates, GABA, has been implicated in both sensory and motor aspects of vocalization in songbirds. To understand the role of GABAergic mechanisms in vocal communication, GABAergic elements must be characterized fully. Hence, we investigated GABA immunohistochemistry in the zebra finch brain, emphasizing auditory areas and song control nuclei. Several nuclei of the ascending auditory pathway showed a moderate to high density of GABAergic neurons including the cochlear nuclei, nucleus laminaris, superior olfactory nucleus, mesencephalic nucleus lateralis pars dorsalis, and nucleus ovoidalis. Telencephalic auditory areas, including field L subfields L1, L2a and L3, as well as the caudomedial nidopallium (NCM) and mesopallium (CMM), contained GABAergic cells at particularly high densities. Considerable GABA labeling was also seen in the shelf area of caudodorsal nidopallium, and the cup area in the arcopallium, as well as in area X, the lateral magnocellular nucleus of the anterior nidopallium, the robust nucleus of the arcopallium and nidopallial nucleus HVC. GABAergic cells were typically small, most likely local inhibitory interneurons, although large GABA-positive cells that were sparsely distributed were also identified. GABA-positive neurites and puncta were identified in most nuclei of the ascending auditory pathway and in song control nuclei. Our data are in accordance with a prominent role of GABAergic mechanisms in regulating the neural circuits involved in song perceptual processing, motor production, and vocal learning in songbirds.

### Keywords

GAD; Avian; NCM; Songbird; Plasticity; HVC

### INTRODUCTION

Gamma-aminobutyric acid (GABA) is the main inhibitory neurotransmitter in the vertebrate brain. GABA-mediated transmission has been implicated in the regulatory control of cellular properties such as neuronal excitability and the statistical likelihood of neuronal firing and of presynaptic neurotransmitter release (Chagnac-Amitai and Connors, 1989a; Chagnac-Amitai

\*Address Correspondence: Raphael Pinaud, PhD, Department of Neurobiology, Duke University Medical Center, Bryan Research Building, room 445A, Durham, NC 27710, Tel: (919) 681-1681, Fax: (919) 681-0877, pinaud@neuro.duke.edu.

<sup>2</sup>Current affiliation: Department of Neurobiology, Duke University Medical Center, Durham, NC, USA

**Publisher's Disclaimer:** This is a PDF file of an unedited manuscript that has been accepted for publication. As a service to our customers we are providing this early version of the manuscript. The manuscript will undergo copyediting, typesetting, and review of the resulting proof before it is published in its final citable form. Please note that during the production process errors may be discovered which could affect the content, and all legal disclaimers that apply to the journal pertain.

and Connors, 1989b; Isaacson et al., 1993; Morrisett et al., 1991; Salin and Prince, 1996; Scanziani et al., 1993; Thompson et al., 1993), as well as in complex network tasks such as the control of sensory receptive field properties (Bolz and Gilbert, 1986; Hata et al., 1988; Sillito, 1977; Sillito, 1979; Sillito and Versiani, 1977; Tremere et al., 2001a; Tremere et al., 2003) and experience-dependent modifications in cortical representation maps (Tremere et al., 2001b; Tremere et al., 2003). Thus, GABAergic transmission impacts the generation of appropriate neural codes required for CNS representations of sensory information about the environment, sensorimotor integration, and motor control programs (Bland and Oddie, 2001; Ramanathan et al., 2002; Werhahn et al., 2002; Ziemann et al., 2001). In most brain areas, GABAergic cells participate in local processing microcircuits, although long-range GABAergic projections have also been described in some systems (Bartlett et al., 2000; Ebner and Armstrong-James, 1990; Jones, 1993; Luo and Perkel, 1999a; Luo and Perkel, 1999b; Peruzzi et al., 1997; Sarter and Bruno, 2002).

We have been investigating the contribution of GABAergic transmission to the central representation of vocal communication signals in songbirds. Songbirds are one of the few animals groups that evolved the ability to learn vocalizations based on an auditory model (Marler et al., 1972; Marler and Waser, 1977). During the sensory acquisition phase of the song learning process, the juvenile hears and memorizes the adult song. During the sensorimotor phase, the bird changes its own vocalizations to match the acquired song template. Intact hearing is crucial for both phases: birds raised in acoustic isolation or deafened fail to develop normal song structure (Konishi, 1965a; Konishi, 1965b; for recent reviews see Zeigler and Marler, 2004), although some exceptions have been noted (Kroodsma et al., 1997; Leitner et al., 2002). Research in zebra finches and canaries have led to major insights into the neuronal basis of vocal learning, in large part because telencephalic areas involved in song auditory processing, production and learning have been identified and their connections mapped in detail (Bottjer et al., 1984; Kelley and Nottebohm, 1979; Mello et al., 1998; Nottebohm and Arnold, 1976; Nottebohm and Arnold, 1979; Nottebohm et al., 1982; Nottebohm et al., 1976; Scharff and Nottebohm, 1991; Vates et al., 1996). As occurs in other avian species and vertebrate groups, the ascending auditory pathway of songbirds is thought to consist of a series of pontine, mesencephalic and thalamic nuclei that convey auditory information from the cochlea to telencephalic centers, although the detailed connectivity of this pathway up to the midbrain has not yet been determined in songbirds (Fig. 1A and B). At the level of the telencephalon, several auditory areas are located within a prominent caudomedial bulge, or lobule (Mello et al., 1998; Vates et al., 1996). These areas include the primary auditory thalamo-recipient zone field L as well as major field L targets, namely the caudomedial nidopallium (NCM) and the caudomedial and caudolateral mesopallium (CMM and CLM, respectively; we use here the revised avian brain nomenclature, as detailed in Reiner et al., 2004). From field L and these primary targets, auditory input reaches other telencephalic areas (Fig. 1B). Although the specific role of individual constituent nuclei or areas has not been clearly established, these central auditory pathways are thought to be crucial for song auditory processing, perception, and possibly the song memorization required for perceptual discrimination and vocal learning (for review, see Mello et al., 2004).

Songbirds also possess a set of interconnected forebrain nuclei known as the song control system that can be subdivided into two main pathways (Fig. 1C). The direct motor pathway is essential for the production of learned vocalizations and includes nidopallial nucleus HVC, the robust nucleus of the arcopallium (RA), and the descending projections of the latter onto the dorsomedial nucleus of the intercollicular complex (DM), the tracheosyringeal component of the hypoglossal nerve (nXIIts), which innervates muscles from the vocal organ (syrinx), and medullary respiratory control centers. The anterior forebrain pathway is essential for song learning and consists of area X of the medial striatum, the medial part of the dorsolateral nucleus of the thalamus (DLM), and the lateral magnocellular nucleus of the anterior nidopallium

(LMAN), which are connected in a circuit organization analogous to mammalian cortico-basal ganglia-thalamo-cortical loops (Bottjer et al., 1989;Nottebohm et al., 1982;Nottebohm et al., 1976; for recent reviews, see Zeigler and Marler, 2004).

GABAergic transmission has been implicated in the physiology of areas involved in both auditory and motor processing of vocalizations in songbirds. For example, GABA antagonism affects synchronized firing within song control nucleus RA and spike properties of projection neurons in nucleus LMAN (Bottjer et al., 1998; Spiro et al., 1999). We have recently used molecular and electrophysiological methods to show that GABAergic cells and synapses are prevalent in telencephalic auditory areas, and that GABAergic neurons show induced expression of the activity-dependent gene *zenk* in response to song auditory stimulation (Pinaud et al., 2004). Thus, inhibitory mechanisms involving GABA appear to participate in the auditory processing, production, and potentially learning of birdsong.

In the present work, we have used an anti-GABA antibody for a detailed characterization of GABAergic elements in auditory and song control areas of the zebra finch brain, to gain further understanding of the neurochemical organization of circuits involved in vocal communication and learning in songbirds. We demonstrate that GABAergic cells and processes are prevalent at several levels of the auditory pathway as well as within song control nuclei. Our observations are consistent with a prominent role of inhibitory mechanisms in the physiology of brain areas that participate in song auditory processing, learning and production in songbirds.

## MATERIAL AND METHODS

### Animals

We used a total of 22 adult zebra finches (*Taeniopygia guttata* - 8 females; 14 males) purchased from a breeder and maintained in our local aviary. Experimental protocols utilized in this study were approved by OHSU's Institutional Animal Care and Use Committee (IACUC) and are in accordance with NIH guidelines. A subset of birds (6 females and 10 males) was maintained overnight in a sound-proof box. The next day, birds were stimulated with a playback of a medley of conspecific songs for 30 minutes, followed by 1 hr of silence and sacrifice (as in Mello and Ribeiro, 1998), in order to test for a possible effect of auditory stimulation on the distribution of GABAergic neurons. All other birds were directly removed from our aviary and immediately sacrificed. Based on a preliminary assessment, we did not observe any evidence that the density of GABAergic neurons was affected by auditory stimulation. Therefore, we combined the control and stimulated groups for the present report.

All birds received an overdose of Nembutal and were quickly perfused transcardially with 10 ml of phosphate-buffered saline (PBS; pH 7.4) followed by 60 ml of a solution containing 1% paraformaldehyde and 2% glutaraldehyde in 0.1 M PBS. A fast and efficient perfusion with saline prior to the fixative was critical for preventing GABA signal from being washed off the tissue. Brains were then dissected out of the skulls, cryoprotected by equilibration in a 30% sucrose solution, included in embedding medium (Tissue-Tek; Sakura Finetek, Torrance, CA), frozen in a dry-ice/propanol bath, cut on a cryostat (20  $\mu$ m thick sections), mounted on glass slides (Fisherbrand Superfrost Plus; Fisher Scientific, Pittsburgh, PA), and stored at -80°C. Most brains were sectioned on the parasagittal plane, although a few brains (n=3) were cut on the frontal plane for comparison.

### Immunohistochemistry (IHC)

We used a commercial rabbit anti-GABA polyclonal antibody (Chemicon International, Temecula, CA; catalog # AB141, immunogen KLH-GABA). Slides were removed from the -80°C freezer and allowed to dry at room temperature (RT) for 30 min. Slides were then

immersed in PB and hydrated for 30 min, followed by incubation for 2 hr at RT in a blocking buffer (BB) that consisted of 0.5% albumin and 0.3% Triton X-100 in 0.1M phosphate buffer (PB; pH 7.4). Sections were then washed for 30 min ( $3 \times 10$  min washes) in PB and incubated overnight at 4°C with the anti-GABA antibody (1:200 dil in BB), in a humid chamber. The slides were then washed for 30 min ( $3 \times 10$  min) in PB and incubated for 2 hr at RT with a biotinylated goat anti-rabbit antibody (1:200 dil in BB; Vector Laboratories, Burlingame, CA). Sections were then washed for 30 min in PB and incubated for 2 hr at RT in avidin-biotin complex (1:100 dil in PB; ABC Elite kit, Vector Laboratories, Burlingame, CA). The slides were then washed for 30 min ( $3 \times 10$  min) in PB and incubated in a filtered solution containing 0.03% diaminobenzidine, 0.15% Nickel sulfate and 0.001% hydrogen peroxide in PB. Sections were periodically monitored for signal under a microscope and reaction was stopped by immersion in PB. The sections were then dehydrated in a standard series of alcohols, delipidized in xylene, and coverslipped.

### Specificity Controls

Omission of the primary antibody resulted in absence of cellular staining, demonstrating the specificity of our IHC detection system (secondary antibody plus ABC reagent). As discussed previously (Grisham and Arnold, 1994), preabsorption of the primary anti-GABA antibody with GABA alone does not block the immunoreactive product detected with this antibody. Rather, to establish the specificity of this antibody, it is necessary to pre-absorb it with GABA conjugated to a carrier protein, analogous to the immunizing molecule used to generate this antibody. We therefore generated a GABA-BSA conjugate as described previously (Walrond et al., 1993), with modifications. We first cross-linked GABA (5 mM) with BSA (5 mg/ml) using glutaraldehyde (at 1% in 0.1 M PB) for 1 hr at RT, under stirring. This solution was then dialyzed against 30 volumes of cold 0.01 M PB (10 volumes/day for 3 days, at 4°C). To pre-absorb the anti-GABA antibody with the conjugate, we incubated the antibody at its working dilution with various concentrations of the post-dialysis conjugate overnight at 4°C under agitation. The pre-absorbed antibody was then used in the IHC procedure. We found that pre-absorption with both 10 µM and 50 µM (but not 1 µM) of the GABA-BSA conjugate successfully and completely abolished GABA-like immunoreactivity in brain sections (Fig. 2B). Further pre-absorption controls using unbound BSA at the same concentrations as for the GABA-BSA conjugate did not alter GABA-like immunoreactivity in our preparations (Fig. 2A). These pre-absorption procedures are in accordance with the J. Comp. Neurol.

recommendations for determining antibody specificity (Saper and Sawchenko, 2003).

### Imaging and Analysis

We used a Nikon E-600 microscope equipped with a motorized stage drive (LEP Mac5000), and coupled to a PC containing the Neurolucida software (Microbrightfield Inc., Colchester, VT) through the Lucivid system for morphometry, or through a digital camera (DVC, Austin, TX) for photomicrograph acquisition. Acquired photomicrographs were transferred to Adobe Photoshop software, where levels were adjusted and illustration plates assembled.

For cell size estimates, we measured the largest linear soma diameter of any given cell using Neurolucida's "Measurement" tool. For each area of interest, we randomly sampled a few hundred neurons in non-overlapping fields throughout the areas investigated, across 3 birds. In Table 1, we represent the absolute values for the largest and smallest soma diameter measured as "Cell Diameter Range" and the "Average Diameter". While it is possible that some subregions of the soma may not have been stained with the anti-GABA antibody, indicating a possible subcellular compartmentalization of GABA distribution, the staining patterns we observed were largely comparable with the cellular staining patterns observed previously for the GABAergic cell marker *zGAD65*, most importantly the clear definition of small and large cell populations (Pinaud et al., 2004). This gives strong indication that the

patterns we have observed and quantified represent well the morphological properties of GABAergic cell somata. Caution is also warranted when considering that some smaller cell diameters quantified in our preparations could represent partial profiles of larger cells that were not fully included in sections analyzed. Even though this possibility would account for minor variations in the estimates obtained for smaller cells, it may have had an effect on estimates for larger cells. However, it is important to consider that the same method was applied throughout the brain and that the estimates reveal clear regional differences in both diameter average and range, including the upper limit of the latter. In many cases such differences are consistent with regional variations in cell size that are also clearly seen by Nissl. This supports the notion that the size estimates described here closely reflect regional differences in cell size.

The quantitative analysis above was performed only in a subset of the birds ( $n=3$  males, brains cut parasagittally) where high quality histological preparations could be obtained for all areas analyzed. A qualitative assessment of the staining patterns indicated that the overall distribution of stained elements throughout the brain and in auditory areas was similar in females in comparison with males. The song control nuclei, which are markedly dimorphic in this species, could not be reliably identified in our IHC preparations of females. Therefore, no attempts were made at quantifying possible sex differences in GABAergic cell distribution.

## RESULTS

To reveal GABAergic cells in the zebra finch brain, we performed IHC with an anti-GABA antibody that has been previously used in this species (Grisham and Arnold, 1994). We could identify labeled cells in most brain areas examined. The majority of these cells was small, most likely representing inhibitory neurons that participate in local networks, as described in other systems. Several areas, however, also contained a small contingent of very large labeled cells. Immunolabeled fibers and punctate staining were also observed in the majority of regions analyzed. The issue of specificity of the anti-GABA antibody we used was previously discussed (Grisham and Arnold, 1994). We have incorporated, however, critical pre-absorption controls (see Methods and Fig. 2) to further establish the specificity of the staining patterns in our preparations. In addition, we examined the labeling in some populations of well-known GABAergic neurons (Batini et al., 1992; Gabbott et al., 1986; Sastry et al., 1997). In the cerebellum, we observed strongly labeled cells in the deep nuclei (Fig. 3A–C). These cells were typically large with strongly-labeled triangular soma (Fig. 3B and C; arrowheads). The Purkinje cells were probably the most heavily labeled cells in the brain (Fig. 3D and E). These cells were markedly large and relatively uniform in size across cerebellar folia. We observed strong immunoreactivity in the soma of virtually all Purkinje cells, and in most cases were able to discern negative cell nuclei (Fig. 3D, arrowheads). We also observed strong labeling over large extensions of the dendritic arborizations of Purkinje cells. These processes could often be followed for a few hundred microns into the molecular layer, where they branched profusely, forming a dense immunoreactive network (Fig. 3D and E). The molecular layer also contained several smaller GABA-positive cells that, based on the location, size and number, likely correspond to basket neurons (Fig. 3D and E, arrows).

Labeled cells were also observed in the globus pallidus (GP). As is characteristic of this area (Churchill and Kalivas, 1994; Smith and Bolam, 1990; Smith et al., 1987), these neurons were very large and relatively sparse, with a predominantly triangular soma and a high density of immunostaining (Fig. 3F and G). Many labeled cells lined up close to the border with the striatum (St), into which they extended prominent immunolabeled dendritic processes that were aligned with the dorso-ventral axis. Such processes were particularly visible in the caudal GP and caudal St (CSt; Fig. 3G, arrows). The dorsal border of the GP could be distinguished due to the very low density of labeled cells in the CSt (Fig. 3F). The GP also contained a high density of uniformly distributed punctate staining.

Thus, known populations of GABAergic neurons are readily and reliably identified in our preparations, and their morphology and distribution are in accordance with previous studies. The staining pattern in the GP also provides further supportive neurochemical evidence for the correspondence between this structure in the avian and mammalian brains, according to the recently revised avian brain nomenclature (Reiner et al, 2004). Below we describe the staining patterns we observed in the nuclei of the ascending auditory pathway, followed by auditory and vocal control areas of the telencephalon. The nuclei in the ascending auditory pathway were identified based on the published pigeon (Karten, 1967) and canary brain atlases (Stokes et al., 1974); the lemniscal nuclei were not examined as they could not be reliably identified in our preparations. All density estimates of GABA-positive cells are relative to the neuronal counts per area based on Nissl-stained adjacent sections. We have processed both hemispheres of all birds included in this study. Although we did not attempt a quantitative assessment, we have observed a similar overall pattern of staining in both hemispheres. All quantifications presented were performed on the left hemispheres.

### Ascending Auditory Pathway

**Nucleus magnocellularis (NM)**—We observed a high density of labeled cells in this nucleus (Fig. 4C and D). These cells were evenly distributed and had predominantly round or ovoid labeled somata with no evident stained neurites. The cells were relatively large (18.2  $\mu\text{m}$  average diameter, 12.2 to 26.4  $\mu\text{m}$  range; Fig. 4D and Table 1), and the majority of them displayed strong immunolabeling, suggesting the presence of high GABA contents (Fig. 4D). A moderate density of punctate staining could be observed, uniformly distributed throughout the extent of NM. It is worth noting that a low level of background staining persisted in this nucleus in the pre-absorption control. This is most likely due to an “edge-of-section” effect, as magnocellularis is located close to the (ventricular) border of the tissue. At any rate, the marked decrease in immunolabeling observed with the pre-absorption argues for the specificity of the staining in NM.

**Nucleus angularis (NA)**—Qualitatively, nucleus angularis had a very low density of labeled cells compared to all other areas in the present study. These cells had an asymmetric distribution, the lowest density occurring laterally and the highest density medially (Fig. 4B), and were moderately small (11.1  $\mu\text{m}$  average diameter, 5.6 to 15.8  $\mu\text{m}$  range; Table 1). The soma morphology varied from round and oval to elongated (Fig. 4F). In addition, immunostaining was mostly confined to the soma but in some cases stained proximal neurites could be seen (Fig. 4F; arrowhead). Strong punctate staining could also be observed in NA, apparently over the somata of unlabeled cells (Fig. 4F).

**Nucleus laminaris (NL)**—Slightly lateral to NM, nucleus laminaris (NL) displayed a moderate density of labeled cells. These cells had an asymmetric distribution, a higher density of immunolabeling perykaria seen laterally and a lower density ventromedially (Fig. 4C). The majority of labeled neurons had ellipsoid and moderately to strongly labeled somata (Fig. 4E, arrows), with no apparent labeled neurites. These cells were relatively small (9.7  $\mu\text{m}$  average diameter, 5.7 to 13.7  $\mu\text{m}$  range; Table 1). We also observed several clusters of coarse labeled puncta over what may represent unlabeled somata (Fig. 4E, arrowheads), suggesting that non-GABAergic cells in this nucleus receive strong GABAergic input.

**Superior olivary nucleus (SON)**—A moderate overall density of labeled cells was detected in this nucleus. Their somata were mostly small (7.6  $\mu\text{m}$  average diameter, 3.9 to 12.4  $\mu\text{m}$  range; Table 1) and their shape varied from round or ovoid to triangular and pyramidal-like (Fig. 5B and C). The cells had moderate staining, but presented strongly labeled and coarse puncta over the soma (Fig. 5C). Such puncta were also distributed over the entire extent of the SON. Larger and more strongly labeled cells were more evident ventrally (Fig. 5B).

**Nucleus mesencephalicus lateralis, pars dorsalis (MLd)**—A relatively high density of GABA-stained cells was observed in this nucleus (Fig. 6B). They had a wide size range (6.7 to 28.4  $\mu\text{m}$  in diameter; Table 1) and marked variation in morphology. Both large neurons with varied soma shapes and small neurons with predominantly round soma were seen (Fig. 6C). Both cell types often exhibited immunopositive neurites that extended from the soma (Fig. 6C; arrowheads) and branched, forming a dense network of labeled processes and punctate staining with a reticular aspect throughout MLd. Interestingly, the strongest staining in both cell types was nuclear, with a more modest labeling seen in the soma (Fig. 6C; arrows). Although a small number of cells with nuclear staining was occasionally seen in other brain areas, the occurrence of such cells was most prominent in MLd. This staining pattern was abolished in our antibody pre-absorption controls, arguing for the specificity of this staining pattern.

**Nucleus ovoidalis (Ov)**—GABA-positive neurons were present both in the core and shell regions of Ov (Fig. 7B). Most of these cells had predominantly round or ellipsoid soma that were strongly labeled (Fig. 7C), and had the smallest soma size compared to all other auditory areas examined (6.7  $\mu\text{m}$  average; Table 1). GABA-positive neurites were rarely seen, except for occasional moderately-stained processes in non-spherical neurons (Fig. 7C, arrowheads). A moderate density of punctate staining was seen throughout the extent of Ov.

### Auditory Areas in the Telencephalon

**Field L (L1, L2a and L3)**—Field L is a large structure, occupying an extensive area of the caudal telencephalon and consisting of several subdivisions. Most of our analysis, including morphometry, was carried out in parasagittal sections approximately 0.9 to 1.0 mm lateral to the midline, where the major field L subdivisions L1, L2a and L3 could be clearly identified based on cytoarchitectonic criteria in Nissl-stained sections adjacent to those reacted for GABA IHC. In addition, the boundaries of L2a could also be defined in GABA immunostained material itself, as labeled cells in this area were organized in a distinct string-like fashion along the dorso-ventral axis. For lack of reliable boundaries in our sections, we did not examine subfield L2b. The caudal boundary of L1 and the rostral boundary of L3 could be easily identified based on the intersection of L2a with the lamina pallialis subpallialis that separates field L from the adjacent CSt. However, the anterior boundary of L1 and the posterior boundary of L3 could not be identified either by Nissl or by IHC.

Relatively high densities of labeled cells were detected in L1, L2a and L3. These cells had a mostly homogeneous distribution at this level of the brain (Fig. 8A). The labeled cells were predominantly round and had a wide size range (4 to 22  $\mu\text{m}$  in diameter; Table 1), but tended to be slightly larger in L2a (13.2  $\mu\text{m}$  average diameter) than in L1 and L3 (9.4 and 10.8  $\mu\text{m}$  average diameter, respectively; Table 1). Cells in all subdivisions had moderately high soma staining; however, very few immunostained processes and puncta were seen. The medial-most part of subdivision L2a could be clearly seen in medial parasagittal sections that also contained NCM and CMM (Fig. 9C). At this level, the large cells in L2a were very strongly labeled, but numerous smaller cells could also be seen.

**Caudomedial Nidopallium (NCM)**—This field L target is also a large and complex area. Our analysis focused on medial parasagittal sections (between 0.7 and 1.0 mm lateral to the midline), where the boundaries of NCM are very distinct (the ventricular zone dorsally, caudally and ventrally, and the lamina mesopallialis, or LaM, and field L2a rostrally). GABA-labeled cells were highly prevalent in NCM. Labeled cells in NCM were evenly distributed (Fig. 9B), with relatively few clusters of 2–4 cells observed (Fig. 9E, arrowhead). Immunoreactive neurons tended to be round or ellipsoid, with strongly stained soma and occasional labeled neurites (Fig. 9E–G). These cells also displayed high variation in diameter and a relatively small average size (Table 1). Qualitatively, they appeared to fall into two

predominant types. The first exhibited small soma (3.3–10  $\mu\text{m}$  diameter range) with varied shapes and pronounced processes (Fig. 9F and G; arrowheads). The second had a larger soma (15–20.8  $\mu\text{m}$  diameter range) with round shape and few processes (Fig. 9F and G; arrows). Both types were present throughout NCM, but the smaller cell type was more prevalent. The larger type was comparable to that seen in adjacent field L2a (Fig. 9C; arrowheads). No apparent punctate staining could be observed in NCM.

**Caudomedial Mesopallium (CMM)**—A relatively high density of GABA-labeled cells could be identified in CMM (Fig. 9D). They were distributed throughout this area, and had a tendency to group into clusters of 3–5 cells (Fig. 9D, arrowheads). Such clusters are typical of CMM, and can be readily identified in sections counterstained for Nissl. GABA-labeled cells in CMM were mainly round or oval and had a wide size range (~4  $\mu\text{m}$  to 19  $\mu\text{m}$  in diameter). The majority of these cells appeared to be small (7  $\mu\text{m}$  average diameter, 4–12  $\mu\text{m}$  range; Table 1), although some larger neurons (15–19  $\mu\text{m}$  diameter range) could also be observed. Immunolabeled cells had relatively high and uniform soma staining, and labeled neurites and punctate staining were rarely seen.

**Nidopallial shelf area**—The dorsal boundary of this field L target corresponds to the ventral boundary of HVC, but its ventral boundary can only be identified with tract-tracing (Vates et al., 1996). Our current analysis was restricted to a 200  $\mu\text{m}$  thick domain immediately ventral to HVC. A modest density of labeled cells could be identified in this region. These cells were distributed along the shelf (Fig. 10B), with no apparent clusters, and had round to ellipsoid somata with strong and homogeneous labeling (Fig. 10D). They tended to be slightly smaller (8.9  $\mu\text{m}$  average diameter; Table 1) compared to the adjacent HVC. Very few neurites were immunolabeled and those did not extend far from the soma. Only low levels of punctate staining were observed.

**Arcopallial cup area**—The internal boundary of the cup area adjacent to song nucleus RA is defined by RA itself, but the external boundary does not exhibit any distinct cytoarchitectonic features and can only be defined by tract-tracing (Mello et al., 1998). Based on the latter, the cup region extends rostroventrally for about 500  $\mu\text{m}$  from the rostroventral boundary of RA. An apparent high density of GABA-positive cells (assessed within 200  $\mu\text{m}$  from the RA boundary) was observed in this region (Fig. 11E and F). These cells were mostly small (7  $\mu\text{m}$  average diameter), had a narrow size range (4.4 to 10.5  $\mu\text{m}$ ; Table 1), and tended to segregate into groups, but not in clusters (Fig. 11F; arrows). The majority displayed a round or ovoid soma that was heavily stained, with no apparent immunolabeled processes (Fig. 11F). Some cells, though, particularly those with moderate staining, had more varied shapes and immunopositive proximal neurites. The cup region also contained lightly immunolabeled processes that formed a modest mesh, as well as a moderately high density of punctate staining.

### Telencephalic Song Control Nuclei

**Nucleus Interfacialis (NIf)**—NIf could be identified in some of our GABA IHC preparations as a small domain embedded between L1, L2a and CSt (Fig. 8A). Compared to the adjacent L1 and L2a, labeled cells in nucleus NIIf were relatively large (9.4  $\mu\text{m}$  average diameter; 3.4 to 16.7  $\mu\text{m}$  range; Table 1). They exhibited relatively strong and uniform soma staining, were uniformly distributed, with no apparent clusters, and had a predominantly round or ovoid soma, although some cells were more elongated (Fig. 8B). Very few processes and little punctate staining could be seen in this area.

**Lateral magnocellular nucleus of the anterior nidopallium (LMAN)**—LMAN boundaries could easily be identified based on GABA IHC staining due to the marked difference in labeled cell sizes between LMAN and the surrounding nidopallium (Fig. 12B).

A modest density of labeled cells could be detected in LMAN. These cells were evenly distributed, with no apparent cell clusters (Fig. 12B). Although labeled cells in LMAN tended to be large (12  $\mu\text{m}$  average diameter), several small labeled neurons could also be seen (5 to 23.8  $\mu\text{m}$  diameter range; Table 1). The small cells tended to have more round or elongated somata compared to the larger cells (Fig. 12C, arrows). The larger cell type displayed highly variable shapes that ranged from oval to more complex types (Fig. 12C, black arrowheads). Most labeled cells exhibited strong immunostaining in the soma and moderate staining of their proximal dendrites (Fig. 12C, white arrowheads). Punctate staining was modest, but more marked in the vicinity of the larger cells.

**Area X of the striatum**—The boundaries of this song nucleus could be easily defined based on the different densities of immunolabeled cells between this region and the surrounding striatum (Figure 13B). A very high density of labeled cells was detected in area X. They were evenly distributed, although a few occasional clusters were seen, and were predominantly small (average diameter 7  $\mu\text{m}$ ; range 3.6 to 22.6  $\mu\text{m}$ ; Table 1). A qualitative evaluation indicated that immunolabeled cells fell into one of two groups: 1) small cells were more numerous and tended to have a round or slightly oval soma (Fig. 13C, arrowheads), and sometime an associated labeled neurite; and 2) large cells (3 to 5 times larger diameter than the smaller cells) were much fewer and had mostly round somata (Figure 13C, arrows). Both types exhibited strong cytoplasmic staining and were evenly distributed. We observed few immunolabeled puncta that were uniformly distributed.

**Nucleus HVC of the nidopallium**—A relatively high density of labeled cells was detected in song nucleus HVC (Fig. 10B). These cells tended to exhibit moderate size (10.7  $\mu\text{m}$  average diameter, 6.7 to 14.3  $\mu\text{m}$  range; Table 1), with a round- or oval-shaped soma (Fig. 10E) and a relatively homogeneous distribution throughout HVC (Fig. 10C and E), instead of being organized into clusters. They displayed strong and homogeneous somatic staining, with very few labeled processes evident. No punctate staining was detected in HVC.

**Robust nucleus of the arcopallium (RA)**—The borders of RA could be easily identified in our preparations because the morphology and size of GABA-labeled cells in RA differed markedly from those in the surrounding arcopallium, and because of a low signal zone demarcating the boundary between RA and the neighboring arcopallium (Fig. 11B, C and E). A high density of labeled cells was observed in RA. These cells tended to be large (14.3  $\mu\text{m}$  average diameter) but had a broad size range (6.4–28.5  $\mu\text{m}$  diameter; Table 1) and were uniformly distributed. Their morphology ranged from cells with round- or oval-shaped somata to pyramidal- and multipolar-like cells (Fig. 11D) and they typically exhibited heavy somatic immunostaining and a negative nucleus (Fig. 11D). Most cells had pronounced labeled processes that extended from the soma and then branched extensively, forming an intricate network throughout RA (Fig. 11D). Despite high neuritic labeling, little punctate staining was observed.

## DISCUSSION

We provide here a detailed account of the distribution of GABAergic elements in auditory processing areas and song control nuclei in the brain of zebra finches. We found that GABA-positive cells are prevalent in several of the examined nuclei of the ascending auditory pathway, in auditory telencephalic areas, and in nuclei of both the anterior and posterior forebrain pathways within the song control system. In addition, GABAergic processes and puncta, presumably corresponding to GABAergic terminals, were observed in a number of these areas. These observations are consistent with the view that GABA plays a significant role in various aspects of birdsong representation, such as song perceptual processing and memorization,

motor control of song production, and vocal learning. Below we discuss the implications of these findings.

### GABAergic Elements in the Ascending Auditory Pathway

The avian ascending auditory pathway has been most extensively investigated in the barn owl, in the context of sound localization, and in chicks, in relation to general auditory physiology. Studies on nuclei angularis (NA) and magnocellularis (NM), which together comprise the avian cochlear nuclei, and nucleus laminaris (NL), thought to correspond to the mammalian medial superior olive (Boord, 1968), have demonstrated a prominent role of GABAergic mechanisms in auditory stimulus processing and encoding. NA encodes the intensity of sound in a series of spike trains, while NM is primarily concerned with temporal properties of the stimulus (Fukui and Ohmori, 2004; Monsivais and Rubel, 2001; Sullivan and Konishi, 1984; Takahashi et al., 1984; Warchol and Dallos, 1990; Young and Rubel, 1983). Projections from NM primarily target NL, where interaural time differences (ITDs) required for sound localization are computed (Carr and Konishi, 1990; Overholt et al., 1992; Young and Rubel, 1983). Patch-clamp recordings in NL have shown that GABAergic inhibition increases coincidence detection of excitatory projections (Funabiki et al., 1998). In addition, the strength of GABA transmission may allow for either an increase or decrease in neuronal excitability in NL (Bruckner and Hyson, 1998). Electrophysiological recordings in the chick, though, indicate that NM is not the primary source of inhibitory input to NL (Zhou and Parks, 1991). Indeed, a GABAergic projection from NM to NL appears to be absent in this species (Bruckner and Hyson, 1998). Robust GABAergic projections in the chick have been described from the superior olfactory nucleus (SON) to both NL and NM (Lachica et al., 1994; Monsivais et al., 2000; Yang et al., 1999), the latter regulating the fidelity of phase-locking of auditory signals (Monsivais et al., 2000). Feedback inhibition from SON onto NL contributes to the temporal integration and coincidence detection required for ITD computations (Yang et al., 1999). Feedback networks that affect auditory processing in NL and NM via the GABAergic projections from SON have been proposed to arise from NA projections to SON, but the neurochemical identity of the latter is not clear (Brainard et al., 1992; Knudsen and Konishi, 1978). In sum, GABAergic influence early in the auditory pathway regulates both gain control and the representation of temporal auditory cues in the cochlear nuclei of non-oscines.

Our findings in the zebra finch are consistent with a prominent role of GABA-mediated inhibition at early stages of the ascending auditory pathway of songbirds. The moderately high density of GABA-positive puncta and neuropil we observed in NM and NL could correspond to the innervation arising from SON. Indeed, relatively large GABAergic cells exist within SON that could correspond to inhibitory projection neurons. Thus, some basic aspects of GABAergic inhibition at the level of cochlear nuclei may be conserved between songbirds and chicks. Our results, however, also provide evidence for the presence of GABAergic cells in both the NM and NL of zebra finches. This finding contrasts with previous reports of very low numbers of such cells in the NM and NL of the chick and barn owl (Code et al., 1989; von Bartheld et al., 1989). Further studies with other GABAergic cell markers in both species would be helpful to further investigate this apparent species difference and to determine its potential impact on the physiology of these nuclei in songbirds. At any rate, significant species differences in the organization and development of the ascending auditory pathways have been previously described in birds. Such differences have been suggested to relate to specializations in auditory processing capabilities and strategies (Kubke and Carr, 2000; Kubke et al., 2004). By analogy, different evolutionary pressures might have contributed to a significantly larger GABAergic influence in the auditory brainstem of songbirds, as compared to other avian species. This neurochemical difference could thus be related to aspects of auditory processing that are of relevance to vocal learning, a behavior not found in the chick and barn owl, the main experimental avian models of brainstem auditory physiology.

GABAergic elements and GABA-mediated inhibition are also prominent at higher levels of the avian ascending auditory pathway. Nucleus MLd in the intercollicular complex (ICo) receives direct projections from SON and from cochlear nuclei, and is considered homologous to the central nucleus of the mammalian inferior colliculus (IC) (Conlee and Parks, 1986). Research in both mammals and birds has shown that GABAergic transmission in the IC controls several aspects of auditory information coding, including the representation of sound intensity and location (Knudsen et al., 2000; Pollak et al., 2003; Sivaramakrishnan et al., 2004; Zheng and Knudsen, 1999). Inhibition through the GABA-A receptor has been shown to participate in the sharpening of auditory tuning-curves in the IC and at other sites along the ascending auditory pathway in both mammals and birds (Chen and Jen, 2000; Suga et al., 1997; Yang et al., 1992). Numerous GABAergic neurons are also present in the medial geniculate body (MGN), the main auditory nucleus of the mammalian thalamus, with significant species differences occurring in the number of such cells (Winer and Larue, 1996). Indeed, it has been suggested that an increase in inhibitory influence in the auditory thalamus across species might correlate with the complex processing required for speech-like communication signals (Winer and Larue, 1996).

Our data demonstrate that numerous GABAergic cells are present in the MLd of zebra finches, and suggest the existence of distinct GABAergic cell types, including small and more numerous cells that likely correspond to local inhibitory interneurons, as well as much larger cells. Interestingly, recent studies have revealed a significant inhibitory projection from the inferior colliculus to the medial geniculate nucleus (MGN) in mammals (Bartlett et al., 2000; Peruzzi et al., 1997; Winer et al., 1995; Winer et al., 1996). In avian species, the equivalent circuitry consists in the projection from MLd to thalamic nucleus Ov, the avian homologue of the ventral division of the mammalian MGN (Brauth et al., 1987; Karten, 1967). While this projection is likely to be predominantly excitatory, it could also contain an inhibitory component originating from putative GABAergic projection neurons in MLd. Consistent with this possibility is our observation that Ov displays a moderate level of GABAergic terminals. Alternatively, such terminals could arise from local connections, or from descending inhibitory projections targeting Ov. Unlike what has been described for the pigeon (Veenman and Reiner, 1994), we observed a high density of GABAergic neurons in Ov, consistent with the possibility that the density of such cells in the auditory thalamus may correlate with the complexity of thalamic auditory processing required for vocal communication (Winer and Larue, 1996). Interestingly, MLd had a high incidence of cells with a nuclear staining pattern. Our specificity controls indicate that this is not an artifactual pattern, but its functional significance is unclear.

Songbirds rely on the auditory processing of complex stimuli for the individual recognition that underlies behaviors such as territoriality, mate selection and courtship (Catchpole and Slater, 1995), as well as for song learning and for the maintenance of the stereotyped adult song (Konishi, 1965a; Leonardo and Konishi, 1999; Nordeen and Nordeen, 1992). Appropriately tuned auditory responses along the auditory pathway likely correlate with the perceptual processing of acoustic features of song. Based on the precedent in mammals (Ehret et al., 2003; Ferragamo et al., 1998; Poirier et al., 2003; Suga et al., 1997; Wenstrup, 1999), we suggest that MLd and Ov in songbirds participate in the shaping of auditory response properties that are relevant to birdsong representation, such as frequency tuning. Songbirds, including zebra finches, can discriminate frequencies with reasonable accuracy, as evidenced by their ability to match their own vocalizations to the tutor's song in the context of vocal learning. More specifically, juveniles gradually shift the fundamental frequency of some syllables to maximize imitation (Tchernichovski et al., 2001). Such a process likely requires plastic changes in brain representations of song and could involve the dense GABAergic networks at the level of MLd and Ov. Although GABAergic inhibition has not been studied in the ascending auditory pathway of songbirds, the high prevalence of GABAergic elements

in zebra finches is consistent with a key role of inhibition in the physiology of this pathway and, thus, in the auditory coding of birdsong.

### GABAergic Elements in Auditory Telencephalic Areas

GABAergic cells were highly abundant in auditory areas of the zebra finch telencephalon and appear to consist of distinct populations of inhibitory neurons. While the smaller cells most likely participate in local circuits, it is possible that at least some of the large cells might represent inhibitory projection neurons, as has been demonstrated for striatal song nucleus area X (Luo and Perkel, 1999a; Luo and Perkel, 1999b). Interestingly, the distribution of large versus small GABAergic cells in the auditory telencephalon was not symmetric. The majority of GABA-positive neurons in field L subfields L1 and L3 belonged to the smaller type, whereas in the thalamo-recipient field L2a, particularly in its medial portion, the larger GABAergic cells were more prevalent. These findings are in accordance with the mRNA distribution of the zebra finch homologue of the 65 kD glutamic-acid decarboxylase (*zGAD65*), the synthetic enzyme for GABA, in auditory areas of zebra finches (Pinaud et al., 2004). *zGAD65*-positive cells also segregate into two populations based on soma size and expression levels of *zGAD65*. While small cells with relatively low *zGAD65* levels are found throughout subfields L1 and L3 and the adjacent NCM and CMM, large neurons with high *zGAD65* levels are found mostly in field L2a, where they are the predominant GABAergic cell type (Pinaud et al., 2004). Further studies are required to determine whether any of the large GABAergic cells in these early auditory telencephalic areas might be projection neurons. We are not aware of any evidence detailing a qualitative distinction of GABAergic cell types in mammalian systems, therefore, it is possible that this feature is unique to the avian brain.

Higher-order auditory areas of the telencephalon are also involved in the auditory processing of birdsong and may play an important role in the formation of song auditory memories (Mello, 2002; Mello et al., 2004). In particular, the caudomedial nidopallium (NCM) and mesopallium (CMM) display robust responses to birdsong auditory stimulation, as revealed by electrophysiological recordings and expression analysis of the activity-dependent gene *zenk* (Chew et al., 1995; Gentner and Margoliash, 2003; Mello and Ribeiro, 1998; Mello et al., 2004; Mello et al., 1992). Until recently, however, very little was known about inhibitory elements in these areas. Based on *in-situ* hybridization for *zGAD65*, we have recently estimated that 36–43% of the neuronal cells in caudomedial auditory structures are GABAergic (Pinaud et al., 2004). Based on a qualitative assessment of the immunocytochemical profile described here, these densities may be even higher than those observed in our previous report (Pinaud et al., 2004). A possible explanation for this discrepancy is that GABAergic cells expressing only the 67kD isoform of GAD were not detected with the *zGAD65* probe, but clarifying this issue awaits molecular probes specific for GAD67. Nonetheless, double *in situ* hybridization has shown that about 42% of the cells that express *zenk* in response to song stimulation express *zGAD65* and are therefore GABAergic (Pinaud et al., 2004). Altogether, these findings provide clear evidence that GABAergic neurons participate in the auditory response to birdsong and suggest that they might contribute to the perceptual processing that underlies song memory formation and vocal-learning.

An intriguing finding of the present work is the high density of GABA-positive neurons in various auditory areas of the songbird telencephalon compared to mammalian auditory areas, where GABAergic cells have been estimated to represent 25–30% of the overall neuronal population, being primarily concentrated in cortical layers 2–4 (Gabbott and Somogyi, 1986; Jones, 1993). It has been proposed that the avian brain, even though lacking for the most part a cortical laminar organization, contains neuronal populations that are comparable to those in various layers of the mammalian cortex (Karten, 1991; Mello et al., 1998; Reiner et al., 2004). Although great caution should be exercised in such a comparison, the various areas that

compose the auditory system may correspond to some extent to the neuronal populations of different layers of the mammalian auditory cortex (Mello et al., 1998; Vates et al., 1996; Wild et al., 1993). For instance, subfield L2a might be analogous to the auditory cortical layer 4, given that it is the main recipient of direct thalamic auditory projections. L2a targets including NCM and CMM appear to be analogous to supragranular layers of auditory cortical areas and arcopallial cells (i.e., cells in the cup region) that originate long descending projections to auditory nuclei would be analogous to infragranular layers. Thus, the caudomedial lobe that encompasses medial field L2a, NCM and CMM may contain an over-representation of cell populations (e.g. GABAergic cells) seen in granular and supragranular layers of the mammalian auditory cortex, should such a correspondence prove correct.

Only vocal learning birds possess telencephalic vocal control nuclei. While the reason may be primarily that vocal learning requires vocal motor representations within telencephalic circuits (see below), it is also possible that vocal control circuits in song learners need to have direct access to information processed in telencephalic auditory areas. Our current data attest to the prominence of GABAergic elements in the latter areas in zebra finches. In addition, experience-dependent plasticity has been described in auditory telencephalic areas, namely song-specific habituation in NCM and experience-dependent changes in unit selectivity in CMM (Chew et al., 1995; Gentner and Margoliash, 2003). Although not directly tested, GABAergic mechanisms could be involved in regulating plasticity and other basic aspects of the physiology of these areas. In fact, patch-clamp recordings of NCM slices have given indication that NCM is under the influence of a powerful inhibitory network at rest, whose action may prevent NCM from runaway excitation upon its activation (Pinaud et al., 2004). Further studies are required to test whether GABAergic influence at this level of the brain can affect perceptual aspects of vocal learning such as the acquisition of song auditory memories or the feedback evaluation of song.

### GABAergic Elements in the Song Control System

The relatively high densities of GABAergic neurons we observed in all song control nuclei suggest that inhibitory transmission is key to the physiology of the song control system. In general, these observations are consistent with the high incidence of GABAergic cells in mammalian pallial and striatal areas, where they provide the major inhibitory component of local processing networks (Gerfen, 1988; Smith and Bolam, 1990; Smith et al., 1987). As in auditory areas, the marked variability we saw in GABAergic soma size in all song nuclei suggests the possible existence of distinct subpopulations of inhibitory cells.

The high density of GABAergic cells in the zebra finch homologue of the basal ganglia, including song nucleus area X, is consistent with the prevalence of GABAergic neurons in the basal ganglia in mammals. Interestingly, area X has mixed striatal and pallidal features, the latter consisting of GABAergic cells that project to thalamic nucleus DLM (Luo and Perkel, 1999a; Luo and Perkel, 1999b). It seems reasonable to suggest that the large GABAergic cells in area X, which were relatively few and sparse, could correspond to the inhibitory neurons that participate in the area X to DLM projection. Both area X and DLM are components of the song system's anterior forebrain pathway, which is implicated in song learning but not in the motor control of song production (Bottjer et al., 1984; Scharff and Nottebohm, 1991; Sohrabji et al., 1990). This pathway is equivalent to mammalian basal ganglia-thalamocortical loops that are involved, among other things, in the learning and performance of movement sequences that require complex sensory-motor integration (Jarvis and Nottebohm, 1997; Jarvis et al., 1998; Simpson and Vicario, 1990; Bottjer et al., 1989; Luo and Perkel, 1999b). We also observed that area X contains a high density of small GABAergic cells. They presumably correspond to GAD-positive cells that do not participate in the X-to-DLM projection (Luo and Perkel, 1999b) and that are thought to be part of local processing networks within area X.

The pallial song control nuclei (LMAN, HVC and RA) also contain several small GABAergic neurons that are most likely local inhibitory cells. Our measurements, however, give indication that GABAergic cell size is predominantly large in all pallial song nuclei. To some extent, this may reflect the generally larger neuronal size in these nuclei as compared with adjacent areas. It is possible, however, that long-range inhibitory projections might not be specific to the anterior forebrain pathway and that at least some of the large GABAergic cells in pallial song nuclei might represent projection neurons. In RA, for instance, some neurons that project to nXIIts are immunopositive for the calcium-binding protein parvalbumin (PV) (Wild et al., 2001). Because PV-positive cells are thought to represent a subpopulation of GABAergic neurons (Reynolds et al., 2004; Reynolds et al., 2001), it is possible that the RA-to-nXIIts projection might be partly GABAergic and thus exert a partly inhibitory effect on this medullary RA target (Wild et al., 2001). This intriguing possibility remains to be determined experimentally. In contrast, recent evidence indicates that the HVC neurons that project to either area X or to RA do not co-express parvalbumin, calbindin or calretinin (Wild et al., 2005). Rather, these calcium-binding proteins appear to define populations of HVC interneurons. Because the three proteins co-localize highly with GABA and together are thought to comprise most or all GABAergic neurons (DeFelipe, 1997), we conclude that the GABAergic cells in HVC are very likely interneurons and not projection neurons.

GABAergic transmission in RA plays a significant role in the generation of appropriate song structure, and has been proposed to regulate the initiation and control of vocal output (Vicario and Raksin, 2000). In addition, the synchronous output from RA projection neurons is thought to be controlled by the activation of local GABAergic interneurons (Spiro et al., 1999). Interestingly, PV-positive cells in the rodent hippocampus have been reported to reliably display fast-firing behavior, while GABAergic cells that express other calcium-binding proteins, namely calbindin and calretinin, do not exhibit consistent firing behavior (Kawaguchi et al., 1987). These observations are of potential relevance to RA physiology, where the fast neuronal firing required to reliably generate song structure could be related to the prominent local GABAergic network described here and to the high density of PV-positive cells (Wild et al., 2001). Similar roles for GABAergic transmission, mediated through GABA-A receptors, have been shown for song nucleus LMAN, where firing behavior is controlled by inhibitory interneurons (Bottjer et al., 1998). Altogether, our current data and the physiological studies discussed above indicate that GABAergic elements are present and prevalent in song control nuclei, and that inhibition plays a significant role in the normal physiology of the song system.

In sum, our data have provided a detailed characterization of GABAergic elements throughout the ascending auditory pathway and song control nuclei of the zebra finch brain. These findings should help in the interpretation of previous anatomical and physiological studies in zebra finches, as well as stimulate future investigations on the properties of inhibitory networks within the songbird brain.

## Acknowledgments

We would like to thank Drs. Liisa Tremere and Jane MacPherson for critical reading of this manuscript and Leatha Lynch for help with the dialysis of the GABA-BSA conjugate. Work was supported by the NIH/NIDCD (grant #02853). Raphael Pinaud is an N.L. Tartar Research Fellow.

## ANATOMICAL ABBREVIATIONS

<b>A</b>	arcopallium
<b>AFP</b>	anterior forebrain pathway
<b>area X</b>	area X of the striatum

<b>Cb</b>	cerebellum
<b>CLM</b>	caudolateral mesopallium
<b>CMM</b>	caudomedial mesopallium
<b>CSt</b>	caudal striatum
<b>DLM</b>	medial part of the dorsolateral nucleus of the thalamus
<b>DM</b>	dorsal medial nucleus of the midbrain
<b>FLM</b>	medial longitudinal fasciculus
<b>GP</b>	globus pallidus
<b>H</b>	hyperpallium
<b>Hp</b>	hippocampus
<b>HVC</b>	nucleus HVC (a letter-based name)
<b>IC</b>	inferior colliculus
<b>ICo</b>	intercollicular nucleus
<b>IV</b>	fourth ventricle
<b>L1</b>	L2a, L3, field L subdivisions
<b>LaM</b>	lamina mesopallialis
<b>LMAN</b>	medial subdivision of the magnocellular nucleus of the anterior nidopallium
<b>M</b>	mesopallium
<b>MLd</b>	dorsal part of the lateral mesencephalic nucleus
<b>MGN</b>	medial geniculate nucleus
<b>N</b>	nidopallium
<b>NA</b>	nucleus angularis
<b>NCM</b>	caudomedial nidopallium
<b>NIf</b>	nucleus interfacialis of the nidopallium
<b>NL</b>	nucleus laminaris
<b>NM</b>	nucleus magnocellularis
<b>nXIIts</b>	tracheosyringeal component of the hypoglossal nerve
<b>Ov</b>	nucleus ovoidalis of the thalamus
<b>P</b>	pons
<b>PFP</b>	posterior forebrain pathway
<b>RA</b>	robust nucleus of the arcopallium
<b>sh</b>	nidopallial shelf region adjacent to HVC

<b>SON</b>	superior olivary nucleus
<b>St</b>	striatum
<b>TeO</b>	optic tectum
<b>Th</b>	thalamus
<b>tOM</b>	occipitomesencephalic tract
<b>V</b>	ventricle
<b>VeL</b>	lateral vestibular nucleus
<b>VII n</b>	nucleus of the seventh cranial (facial) nerve

## References

- Bartlett EL, Stark JM, Guillory RW, Smith PH. Comparison of the fine structure of cortical and collicular terminals in the rat medial geniculate body. *Neuroscience* 2000;100(4):811–828. [PubMed: 11036215]
- Batini C, Compion C, Buisseret-Delmas C, Daniel H, Guegan M. Cerebellar nuclei and the nucleocortical projections in the rat: retrograde tracing coupled to GABA and glutamate immunohistochemistry. *J Comp Neurol* 1992;315(1):74–84. [PubMed: 1371781]
- Bland BH, Oddie SD. Theta band oscillation and synchrony in the hippocampal formation and associated structures: the case for its role in sensorimotor integration. *Behav Brain Res* 2001;127(1–2):119–136. [PubMed: 11718888]
- Bolz J, Gilbert CD. Generation of end-inhibition in the visual cortex via interlaminar connections. *Nature* 1986;320(6060):362–365. [PubMed: 3960119]
- Boord RL. Ascending projections of the primary cochlear nuclei and nucleus laminaris in the pigeon. *J Comp Neurol* 1968;133(4):523–541. [PubMed: 4185132]
- Bottjer SW, Brady JD, Walsh JP. Intrinsic and synaptic properties of neurons in the vocal-control nucleus IMAN from in vitro slice preparations of juvenile and adult zebra finches. *J Neurobiol* 1998;37(4):642–658. [PubMed: 9858265]
- Bottjer SW, Halsema KA, Brown SA, Miesner EA. Axonal connections of a forebrain nucleus involved with vocal learning in zebra finches. *J Comp Neurol* 1989;279(2):312–326. [PubMed: 2464011]
- Bottjer SW, Miesner EA, Arnold AP. Forebrain lesions disrupt development but not maintenance of song in passerine birds. *Science* 1984;224(4651):901–903. [PubMed: 6719123]
- Brainard MS, Knudsen EI, Esterly SD. Neural derivation of sound source location: resolution of spatial ambiguities in binaural cues. *J Acoust Soc Am* 1992;91(2):1015–1027. [PubMed: 1556303]
- Brauth SE, McHale CM, Brasher CA, Dooling RJ. Auditory pathways in the budgerigar. I. Thalamo-telencephalic projections. *Brain Behav Evol* 1987;30(3–4):174–199. [PubMed: 3664262]
- Bruckner S, Hyson RL. Effect of GABA on the processing of interaural time differences in nucleus laminaris neurons in the chick. *Eur J Neurosci* 1998;10(11):3438–3450. [PubMed: 9824457]
- Carr CE, Konishi M. A circuit for detection of interaural time differences in the brain stem of the barn owl. *J Neurosci* 1990;10(10):3227–3246. [PubMed: 2213141]
- Chagnac-Amitai Y, Connors BW. Horizontal spread of synchronized activity in neocortex and its control by GABA-mediated inhibition. *J Neurophysiol* 1989a;61(4):747–758. [PubMed: 2542471]
- Chagnac-Amitai Y, Connors BW. Synchronized excitation and inhibition driven by intrinsically bursting neurons in neocortex. *J Neurophysiol* 1989b;62(5):1149–1162. [PubMed: 2585046]
- Chen QC, Jen PH. Bicuculline application affects discharge patterns, rate-intensity functions, and frequency tuning characteristics of bat auditory cortical neurons. *Hear Res* 2000;150(1–2):161–174. [PubMed: 11077201]
- Chew SJ, Mello C, Nottebohm F, Jarvis E, Vicario DS. Decrements in auditory responses to a repeated conspecific song are long-lasting and require two periods of protein synthesis in the songbird forebrain. *Proc Natl Acad Sci U S A* 1995;92(8):3406–3410. [PubMed: 7724575]

- Churchill L, Kalivas PW. A topographically organized gamma-aminobutyric acid projection from the ventral pallidum to the nucleus accumbens in the rat. *J Comp Neurol* 1994;345(4):579–595. [PubMed: 7962701]
- Code RA, Burd GD, Rubel EW. Development of GABA immunoreactivity in brainstem auditory nuclei of the chick: ontogeny of gradients in terminal staining. *J Comp Neurol* 1989;284(4):504–518. [PubMed: 2768549]
- Coggeshall RE, Lekan HA. Methods for determining numbers of cells and synapses: a case for more uniform standards of review. *J Comp Neurol* 1996;364(1):6–15. [PubMed: 8789272]
- Conlee JW, Parks TN. Origin of ascending auditory projections to the nucleus mesencephalicus lateralis pars dorsalis in the chicken. *Brain Res* 1986;367(1–2):96–113. [PubMed: 3697720]
- Ebner FF, Armstrong-James MA. Intracortical processes regulating the integration of sensory information. *Prog Brain Res* 1990;86:129–141. [PubMed: 1982365]
- Ehret G, Egorova M, Hage SR, Muller BA. Spatial map of frequency tuning-curve shapes in the mouse inferior colliculus. *Neuroreport* 2003;14(10):1365–1369. [PubMed: 12876475]
- Ferragamo MJ, Haresign T, Simmons JA. Frequency tuning, latencies, and responses to frequency-modulated sweeps in the inferior colliculus of the echolocating bat, *Eptesicus fuscus*. *J Comp Physiol [A]* 1998;182(1):65–79.
- Fukui I, Ohmori H. Tonotopic gradients of membrane and synaptic properties for neurons of the chicken nucleus magnocellularis. *J Neurosci* 2004;24(34):7514–7523. [PubMed: 15329398]
- Funabiki K, Koyano K, Ohmori H. The role of GABAergic inputs for coincidence detection in the neurones of nucleus laminaris of the chick. *J Physiol* 1998;508 (Pt 3):851–869. [PubMed: 9518738]
- Gabbott PL, Somogyi J, Stewart MG, Hamori J. GABA-immunoreactive neurons in the rat cerebellum: a light and electron microscope study. *J Comp Neurol* 1986;251(4):474–490. [PubMed: 3537020]
- Gabbott PL, Somogyi P. Quantitative distribution of GABA-immunoreactive neurons in the visual cortex (area 17) of the cat. *Exp Brain Res* 1986;61(2):323–331. [PubMed: 3005016]
- Gentner TQ, Margoliash D. Neuronal populations and single cells representing learned auditory objects. *Nature* 2003;424(6949):669–674. [PubMed: 12904792]
- Gerfen CR. Synaptic organization of the striatum. *J Electron Microsc Tech* 1988;10(3):265–281. [PubMed: 3069970]
- Grisham W, Arnold AP. Distribution of GABA-like immunoreactivity in the song system of the zebra finch. *Brain Res* 1994;651(1–2):115–122. [PubMed: 7922557]
- Hata Y, Tsumoto T, Sato H, Hagiwara K, Tamura H. Inhibition contributes to orientation selectivity in visual cortex of cat. *Nature* 1988;335(6193):815–817. [PubMed: 3185710]
- Isaacson JS, Solis JM, Nicoll RA. Local and diffuse synaptic actions of GABA in the hippocampus. *Neuron* 1993;10(2):165–175. [PubMed: 7679913]
- Jarvis ED, Nottebohm F. Motor-driven gene expression. *Proc Natl Acad Sci U S A* 1997;94(8):4097–4102. [PubMed: 9108111]
- Jarvis ED, Scharff C, Grossman MR, Ramos JA, Nottebohm F. For whom the bird sings: context-dependent gene expression. *Neuron* 1998;21(4):775–788. [PubMed: 9808464]
- Jones EG. GABAergic neurons and their role in cortical plasticity in primates. *Cereb Cortex* 1993;3(5):361–372. [PubMed: 8260806]
- Karten HJ. The organization of the ascending auditory pathway in the pigeon (*Columba livia*). I. Diencephalic projections of the inferior colliculus (nucleus mesencephali lateralis, pars dorsalis). *Brain Res* 1967;6(3):409–427. [PubMed: 6076249]
- Karten HJ. The ascending auditory pathway in the pigeon (*Columba livia*). II. Telencephalic projections of the nucleus ovoidalis thalami. *Brain Res* 1968;11(1):134–153. [PubMed: 5749228]
- Karten HJ. Homology and evolutionary origins of the ‘neocortex’. *Brain Behav Evol* 1991;38(4–5):264–272. [PubMed: 1777808]
- Kawaguchi Y, Katsumaru H, Kosaka T, Heizmann CW, Hama K. Fast spiking cells in rat hippocampus (CA1 region) contain the calcium-binding protein parvalbumin. *Brain Res* 1987;416(2):369–374. [PubMed: 3304536]
- Kelley DB, Nottebohm F. Projections of a telencephalic auditory nucleus-field L-in the canary. *J Comp Neurol* 1979;183(3):455–469. [PubMed: 759444]

- Knudsen EI, Konishi M. Space and frequency are represented separately in auditory midbrain of the owl. *J Neurophysiol* 1978;41(4):870–884. [PubMed: 681991]
- Knudsen EI, Zheng W, DeBello WM. Traces of learning in the auditory localization pathway. *Proc Natl Acad Sci U S A* 2000;97(22):11815–11820. [PubMed: 11050214]
- Konishi M. Effects of deafening on song development in American robins and black-headed grosbeaks. *Z Tierpsychol* 1965a;22(5):584–599. [PubMed: 5879978]
- Konishi M. The role of auditory feedback in the control of vocalization in the white-crowned sparrow. *Z Tierpsychol* 1965b;22(7):770–783. [PubMed: 5874921]
- Kroodsma DE, Houlihan PW, Fallon PA, Wells JA. Song development by grey catbirds. *Anim Behav* 1997;54(2):457–464. [PubMed: 9268478]
- Kubke MF, Carr CE. Development of the auditory brainstem of birds: comparison between barn owls and chickens. *Hear Res* 2000;147(1–2):1–20. [PubMed: 10962169]
- Kubke MF, Massoglia DP, Carr CE. Bigger brains or bigger nuclei? Regulating the size of auditory structures in birds. *Brain Behav Evol* 2004;63(3):169–180. [PubMed: 14726625]
- Lachica EA, Rubsam R, Rubel EW. GABAergic terminals in nucleus magnocellularis and laminaris originate from the superior olfactory nucleus. *J Comp Neurol* 1994;348(3):403–418. [PubMed: 7844255]
- Leitner S, Nicholson J, Leisler B, DeVoejd TJ, Catchpole CK. Song and the song control pathway in the brain can develop independently of exposure to song in the sedge warbler. *Proc R Soc Lond B Biol Sci* 2002;269(1509):2519–2524.
- Leonardo A, Konishi M. Decrystallization of adult birdsong by perturbation of auditory feedback. *Nature* 1999;399(6735):466–470. [PubMed: 10365958]
- Levin MD, Kubke MF, Schneider M, Wentholt R, Carr CE. Localization of AMPA-selective glutamate receptors in the auditory brainstem of the barn owl. *J Comp Neurol* 1997;378(2):239–253. [PubMed: 9120063]
- Luo M, Perkel DJ. A GABAergic, strongly inhibitory projection to a thalamic nucleus in the zebra finch song system. *J Neurosci* 1999a;19(15):6700–6711. [PubMed: 10414999]
- Luo M, Perkel DJ. Long-range GABAergic projection in a circuit essential for vocal learning. *J Comp Neurol* 1999b;403(1):68–84. [PubMed: 10075444]
- Marler P, Mundinger P, Waser MS, Lutjen A. Effects of acoustical stimulation and deprivation on song development in red-winged blackbirds (*Agelaius phoeniceus*). *Anim Behav* 1972;20(3):586–606. [PubMed: 4661310]
- Marler P, Waser MS. Role of auditory feedback in canary song development. *J Comp Physiol Psychol* 1977;91(1):8–16. [PubMed: 838918]
- Mello CV. Mapping vocal communication pathways in birds with inducible gene expression. *J Comp Physiol A Neuroethol Sens Neural Behav Physiol* 2002;188(11–12):943–959. [PubMed: 12471493]
- Mello CV, Ribeiro S. ZENK protein regulation by song in the brain of songbirds. *J Comp Neurol* 1998;393(4):426–438. [PubMed: 9550149]
- Mello CV, Vates GE, Okuhata S, Nottebohm F. Descending auditory pathways in the adult male zebra finch (*Taeniopygia guttata*). *J Comp Neurol* 1998;395(2):137–160. [PubMed: 9603369]
- Mello CV, Velho TA, Pinaud R. Song-induced gene expression: a window on song auditory processing and perception. *Ann N Y Acad Sci* 2004;1016:263–281. [PubMed: 15313780]
- Mello CV, Vicario DS, Clayton DF. Song presentation induces gene expression in the songbird forebrain. *Proc Natl Acad Sci U S A* 1992;89(15):6818–6822. [PubMed: 1495970]
- Monsivais P, Rubel EW. Accommodation enhances depolarizing inhibition in central neurons. *J Neurosci* 2001;21(19):7823–7830. [PubMed: 11567073]
- Monsivais P, Yang L, Rubel EW. GABAergic inhibition in nucleus magnocellularis: implications for phase locking in the avian auditory brainstem. *J Neurosci* 2000;20(8):2954–2963. [PubMed: 10751448]
- Morrisett RA, Mott DD, Lewis DV, Swartzwelder HS, Wilson WA. GABAB-receptor-mediated inhibition of the N-methyl-D-aspartate component of synaptic transmission in the rat hippocampus. *J Neurosci* 1991;11(1):203–209. [PubMed: 1846009]

- Nordeen KW, Nordeen EJ. Auditory feedback is necessary for the maintenance of stereotyped song in adult zebra finches. *Behav Neural Biol* 1992;57(1):58–66. [PubMed: 1567334]
- Nottebohm F, Arnold AP. Sexual dimorphism in vocal control areas of the songbird brain. *Science* 1976;194(4261):211–213. [PubMed: 959852]
- Nottebohm F, Arnold AP. Songbirds' brains: sexual dimorphism. *Science* 1979;206(4420):769. [PubMed: 493981]
- Nottebohm F, Kelley DB, Paton JA. Connections of vocal control nuclei in the canary telencephalon. *J Comp Neurol* 1982;207(4):344–357. [PubMed: 7119147]
- Nottebohm F, Stokes TM, Leonard CM. Central control of song in the canary, *Serinus canarius*. *J Comp Neurol* 1976;165(4):457–486. [PubMed: 1262540]
- Overholt EM, Rubel EW, Hyson RL. A circuit for coding interaural time differences in the chick brainstem. *J Neurosci* 1992;12(5):1698–1708. [PubMed: 1578264]
- Parks TN, Rubel EW. Organization and development of brain stem auditory nuclei of the chicken: organization of projections from n. magnocellularis to n. laminaris. *J Comp Neurol* 1975;164(4):435–448. [PubMed: 1206128]
- Parks TN, Rubel EW. Organization and development of the brain stem auditory nuclei of the chicken: primary afferent projections. *J Comp Neurol* 1978;180(3):439–448. [PubMed: 659669]
- Peruzzi D, Bartlett E, Smith PH, Oliver DL. A monosynaptic GABAergic input from the inferior colliculus to the medial geniculate body in rat. *J Neurosci* 1997;17(10):3766–3777. [PubMed: 9133396]
- Pinaud R, Velho TA, Jeong JK, Tremere LA, Leao RM, von Gersdorff H, Mello CV. GABAergic neurons participate in the brain's response to birdsong auditory stimulation. *Eur J Neurosci* 2004;20(5):1318–1330. [PubMed: 15341603]
- Poirier P, Samson FK, Imig TJ. Spectral shape sensitivity contributes to the azimuth tuning of neurons in the cat's inferior colliculus. *J Neurophysiol* 2003;89(5):2760–2777. [PubMed: 12740413]
- Pollak GD, Burger RM, Klug A. Dissecting the circuitry of the auditory system. *Trends Neurosci* 2003;26(1):33–39. [PubMed: 12495861]
- Ramanathan S, Hanley JJ, Deniau JM, Bolam JP. Synaptic convergence of motor and somatosensory cortical afferents onto GABAergic interneurons in the rat striatum. *J Neurosci* 2002;22(18):8158–8169. [PubMed: 12223570]
- Reiner A, Perkel DJ, Bruce LL, Butler AB, Csillag A, Kuenzel W, Medina L, Paxinos G, Shimizu T, Striedter G, Wild M, Ball GF, Durand S, Gunturkun O, Lee DW, Mello CV, Powers A, White SA, Hough G, Kubikova L, Smulders TV, Wada K, Dugas-Ford J, Husband S, Yamamoto K, Yu J, Siang C, Jarvis ED, Guturkun O. Revised nomenclature for avian telencephalon and some related brainstem nuclei. *J Comp Neurol* 2004;473(3):377–414. [PubMed: 15116397]
- Reynolds GP, Abdul-Monim Z, Neill JC, Zhang ZJ. Calcium binding protein markers of GABA deficits in schizophrenia--postmortem studies and animal models. *Neurotox Res* 2004;6(1):57–61. [PubMed: 15184106]
- Reynolds GP, Zhang ZJ, Beasley CL. Neurochemical correlates of cortical GABAergic deficits in schizophrenia: selective losses of calcium binding protein immunoreactivity. *Brain Res Bull* 2001;55(5):579–584. [PubMed: 11576754]
- Rubel EW, Parks TN. Organization and development of brain stem auditory nuclei of the chicken: tonotopic organization of n. magnocellularis and n. laminaris. *J Comp Neurol* 1975;164(4):411–433. [PubMed: 1206127]
- Salin PA, Prince DA. Spontaneous GABA<sub>A</sub> receptor-mediated inhibitory currents in adult rat somatosensory cortex. *J Neurophysiol* 1996;75(4):1573–1588. [PubMed: 8727397]
- Saper CB. Any way you cut it: a new journal policy for the use of unbiased counting methods. *J Comp Neurol* 1996;364(1):5. [PubMed: 8789271]
- Saper CB, Sawchenko PE. Magic peptides, magic antibodies: guidelines for appropriate controls for immunohistochemistry. *J Comp Neurol* 2003;465(2):161–163. [PubMed: 12949777]
- Sarter M, Bruno JP. The neglected constituent of the basal forebrain corticopetal projection system: GABAergic projections. *Eur J Neurosci* 2002;15(12):1867–1873. [PubMed: 12099892]
- Sastray BR, Morishita W, Yip S, Shew T. GABA-ergic transmission in deep cerebellar nuclei. *Prog Neurobiol* 1997;53(2):259–271. [PubMed: 9364613]

- Scanziani M, Gahwiler BH, Thompson SM. Presynaptic inhibition of excitatory synaptic transmission mediated by alpha adrenergic receptors in area CA3 of the rat hippocampus in vitro. *J Neurosci* 1993;13(12):5393–5401. [PubMed: 7504723]
- Scharff C, Nottebohm F. A comparative study of the behavioral deficits following lesions of various parts of the zebra finch song system: implications for vocal learning. *J Neurosci* 1991;11(9):2896–2913. [PubMed: 1880555]
- Sillito AM. Inhibitory processes underlying the directional specificity of simple, complex and hypercomplex cells in the cat's visual cortex. *J Physiol* 1977;271(3):699–720. [PubMed: 926020]
- Sillito AM. Inhibitory mechanisms influencing complex cell orientation selectivity and their modification at high resting discharge levels. *J Physiol* 1979;289:33–53. [PubMed: 458666]
- Sillito AM, Versiani V. The contribution of excitatory and inhibitory inputs to the length preference of hypercomplex cells in layers II and III of the cat's striate cortex. *J Physiol* 1977;273(3):775–790. [PubMed: 604458]
- Simpson HB, Vicario DS. Brain pathways for learned and unlearned vocalizations differ in zebra finches. *J Neurosci* 1990;10(5):1541–1556. [PubMed: 2332796]
- Sivaramakrishnan S, Sterbing-D'Angelo SJ, Filipovic B, D'Angelo WR, Oliver DL, Kuwada S. GABA (A) synapses shape neuronal responses to sound intensity in the inferior colliculus. *J Neurosci* 2004;24(21):5031–5043. [PubMed: 15163696]
- Smith Y, Bolam JP. The output neurones and the dopaminergic neurones of the substantia nigra receive a GABA-containing input from the globus pallidus in the rat. *J Comp Neurol* 1990;296(1):47–64. [PubMed: 1694189]
- Smith Y, Parent A, Seguela P, Descarries L. Distribution of GABA-immunoreactive neurons in the basal ganglia of the squirrel monkey (*Saimiri sciureus*). *J Comp Neurol* 1987;259(1):50–64. [PubMed: 3294929]
- Sohrabji F, Nordeen EJ, Nordeen KW. Selective impairment of song learning following lesions of a forebrain nucleus in the juvenile zebra finch. *Behav Neural Biol* 1990;53(1):51–63. [PubMed: 2302141]
- Spiro JE, Dalva MB, Mooney R. Long-range inhibition within the zebra finch song nucleus RA can coordinate the firing of multiple projection neurons. *J Neurophysiol* 1999;81(6):3007–3020. [PubMed: 10368416]
- Stokes TM, Leonard CM, Nottebohm F. The telencephalon, diencephalon, and mesencephalon of the canary, *Serinus canaria*, in stereotaxic coordinates. *J Comp Neurol* 1974;156(3):337–374. [PubMed: 4609173]
- Suga N, Zhang Y, Yan J. Sharpening of frequency tuning by inhibition in the thalamic auditory nucleus of the mustached bat. *J Neurophysiol* 1997;77(4):2098–2114. [PubMed: 9114258]
- Sullivan WE, Konishi M. Segregation of stimulus phase and intensity coding in the cochlear nucleus of the barn owl. *J Neurosci* 1984;4(7):1787–1799. [PubMed: 6737041]
- Takahashi T, Moiseff A, Konishi M. Time and intensity cues are processed independently in the auditory system of the owl. *J Neurosci* 1984;4(7):1781–1786. [PubMed: 6737040]
- Takahashi TT, Konishi M. Projections of nucleus angularis and nucleus laminaris to the lateral lemniscal nuclear complex of the barn owl. *J Comp Neurol* 1988;274(2):212–238. [PubMed: 2463287]
- Tchernichovski O, Mitra PP, Lints T, Nottebohm F. Dynamics of the vocal imitation process: how a zebra finch learns its song. *Science* 2001;291(5513):2564–2569. [PubMed: 11283361]
- Thompson SM, Capogna M, Scanziani M. Presynaptic inhibition in the hippocampus. *Trends Neurosci* 1993;16(6):222–227. [PubMed: 7688163]
- Tremere L, Hicks TP, Rasmusson DD. Expansion of receptive fields in raccoon somatosensory cortex *in vivo* by GABA(A) receptor antagonism: implications for cortical reorganization. *Exp Brain Res* 2001a;136(4):447–455. [PubMed: 11291725]
- Tremere L, Hicks TP, Rasmusson DD. Role of inhibition in cortical reorganization of the adult raccoon revealed by microiontophoretic blockade of GABA(A) receptors. *J Neurophysiol* 2001b;86(1):94–103. [PubMed: 11431491]
- Tremere, LA.; Pinaud, R.; De Weerd, P. Contributions of inhibitory mechanisms to perceptual completion and cortical reorganization. In: Pessoa, L.; De Weerd, P., editors. *Filling-in: from perceptual completion to cortical reorganization*. New York: Oxford University Press; 2003. p. 295–322.

- Vates GE, Broome BM, Mello CV, Nottebohm F. Auditory pathways of caudal telencephalon and their relation to the song system of adult male zebra finches. *J Comp Neurol* 1996;366(4):613–642. [PubMed: 8833113]
- Veenman CL, Reiner A. The distribution of GABA-containing perikarya, fibers, and terminals in the forebrain and midbrain of pigeons, with particular reference to the basal ganglia and its projection targets. *J Comp Neurol* 1994;339(2):209–250. [PubMed: 8300906]
- Vicario DS, Raksin JN. Possible roles for GABAergic inhibition in the vocal control system of the zebra finch. *Neuroreport* 2000;11(16):3631–3635. [PubMed: 11095533]
- von Bartheld CS, Code RA, Rubel EW. GABAergic neurons in brainstem auditory nuclei of the chick: distribution, morphology, and connectivity. *J Comp Neurol* 1989;287(4):470–483. [PubMed: 2477407]
- Walrond JP, Govind CK, Huestis SE. Two structural adaptations for regulating transmitter release at lobster neuromuscular synapses. *J Neurosci* 1993;13(11):4831–4845. [PubMed: 8229201]
- Warchol ME, Dallos P. Neural coding in the chick cochlear nucleus. *J Comp Physiol [A]* 1990;166(5):721–734.
- Wenstrup JJ. Frequency organization and responses to complex sounds in the medial geniculate body of the mustached bat. *J Neurophysiol* 1999;82(5):2528–2544. [PubMed: 10561424]
- Werhahn KJ, Mortensen J, Kaelin-Lang A, Boroojerdi B, Cohen LG. Cortical excitability changes induced by deafferentation of the contralateral hemisphere. *Brain* 2002;125(Pt 6):1402–1413. [PubMed: 12023328]
- Wild JM, Karten HJ, Frost BJ. Connections of the auditory forebrain in the pigeon (*Columba livia*). *J Comp Neurol* 1993;337(1):32–62. [PubMed: 8276991]
- Wild JM, Williams MN, Suthers RA. Parvalbumin-positive projection neurons characterise the vocal premotor pathway in male, but not female, zebra finches. *Brain Res* 2001;917(2):235–252. [PubMed: 11640910]
- Winer JA, Larue DT. Evolution of GABAergic circuitry in the mammalian medial geniculate body. *Proc Natl Acad Sci U S A* 1996;93(7):3083–3087. [PubMed: 8610172]
- Winer JA, Larue DT, Pollak GD. GABA and glycine in the central auditory system of the mustache bat: structural substrates for inhibitory neuronal organization. *J Comp Neurol* 1995;355(3):317–353. [PubMed: 7636017]
- Winer JA, Saint Marie RL, Larue DT, Oliver DL. GABAergic feedforward projections from the inferior colliculus to the medial geniculate body. *Proc Natl Acad Sci U S A* 1996;93(15):8005–8010. [PubMed: 8755593]
- Yang L, Monsivais P, Rubel EW. The superior olfactory nucleus and its influence on nucleus laminaris: a source of inhibitory feedback for coincidence detection in the avian auditory brainstem. *J Neurosci* 1999;19(6):2313–2325. [PubMed: 10066281]
- Yang L, Pollak GD, Resler C. GABAergic circuits sharpen tuning curves and modify response properties in the mustache bat inferior colliculus. *J Neurophysiol* 1992;68(5):1760–1774. [PubMed: 1479443]
- Young SR, Rubel EW. Frequency-specific projections of individual neurons in chick brainstem auditory nuclei. *J Neurosci* 1983;3(7):1373–1378. [PubMed: 6864252]
- Zeigler, HP.; Marler, P. Behavioral Neurobiology of Birdsong. New York: New York Academy of Sciences; 2004.
- Zheng W, Knudsen EI. Functional selection of adaptive auditory space map by GABA-mediated inhibition. *Science* 1999;284(5416):962–965. [PubMed: 10320376]
- Ziemann U, Muellbacher W, Hallett M, Cohen LG. Modulation of practice-dependent plasticity in human motor cortex. *Brain* 2001;124(Pt 6):1171–1181. [PubMed: 11353733]

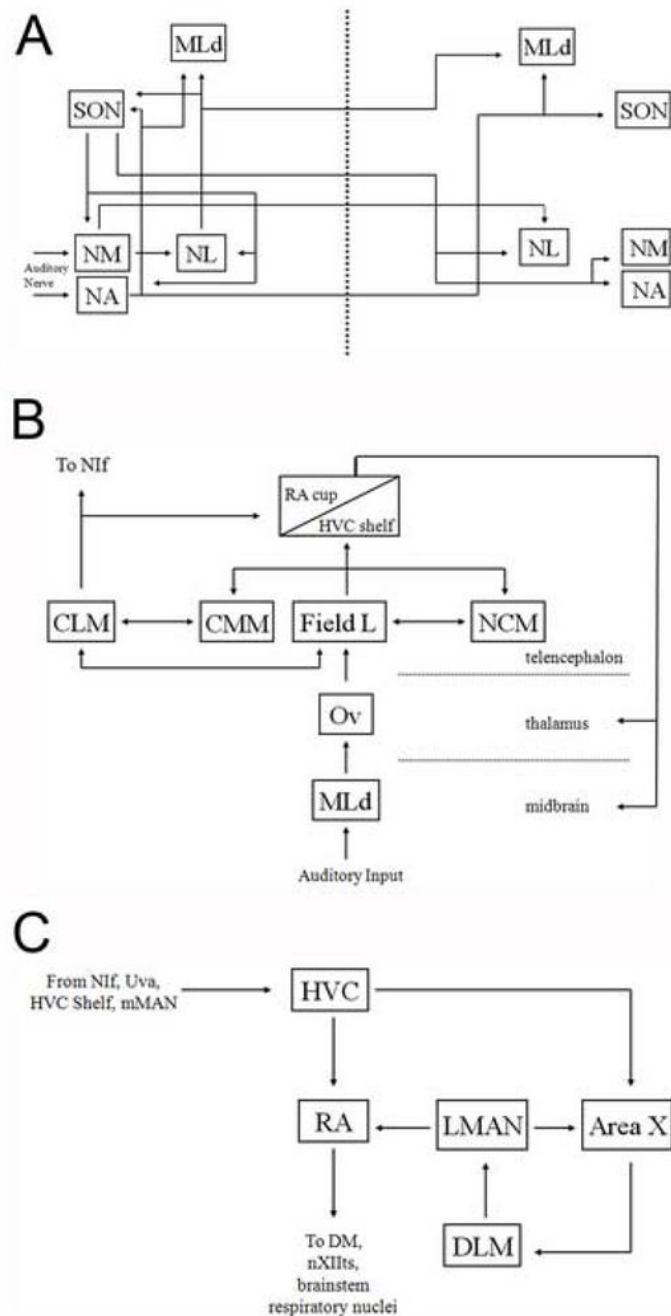


**Figure 1. The ascending auditory pathway and the song control system of songbirds**

(A) Diagram of the main nuclei and connections of the auditory pathways, up to the midbrain. Dotted line represents the midline. (B) Diagram of the auditory pathways from the midbrain to the telencephalon, and intratelencephalic projections. (C) Diagram of the song control system. For clarity, only the main nuclei and projections are shown in all diagrams, and only unilateral projections in (B) and (C). (A) is mostly based on work conducted in non-oscine species like chicks and the barn owl (Lachica et al., 1994; Levin et al., 1997; Parks and Rubel, 1975; Parks and Rubel, 1978; Rubel and Parks, 1975; Takahashi and Konishi, 1988), whereas (B) and (C) is supported by data obtained in zebra finches and canaries, as well as non-oscine species like the pigeon, chicks and budgerigars (Bottjer et al., 1984; Brauth et al., 1987; Karten,

1967; Karten, 1968; Nottebohm et al., 1976; Parks and Rubel, 1975; Parks and Rubel, 1978). For abbreviations, see list.

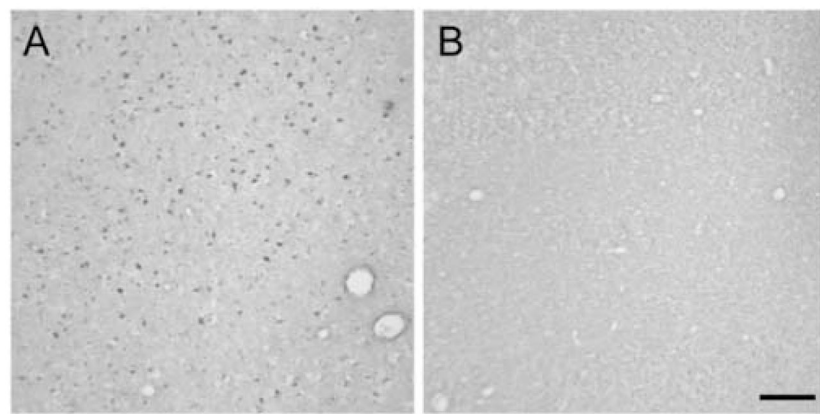


**Figure 2. Specificity of GABA immunoreactivity in the zebra finch brain**

(A) Low power photomicrograph depicting GABA-like immunoreactivity in the nidopallium of a male zebra finch. This section was incubated with the anti-GABA antibody that was pre-absorbed with 50  $\mu$ M of unbound BSA. (B) Photomicrograph of a section incubated with the anti-GABA antibody pre-absorbed with 50  $\mu$ M of the GABA-BSA conjugate (see Material and Methods). Note that GABA-like immunoreactivity was completely abolished after the antibody pre-absorption. Scale bar = 100  $\mu$ m.

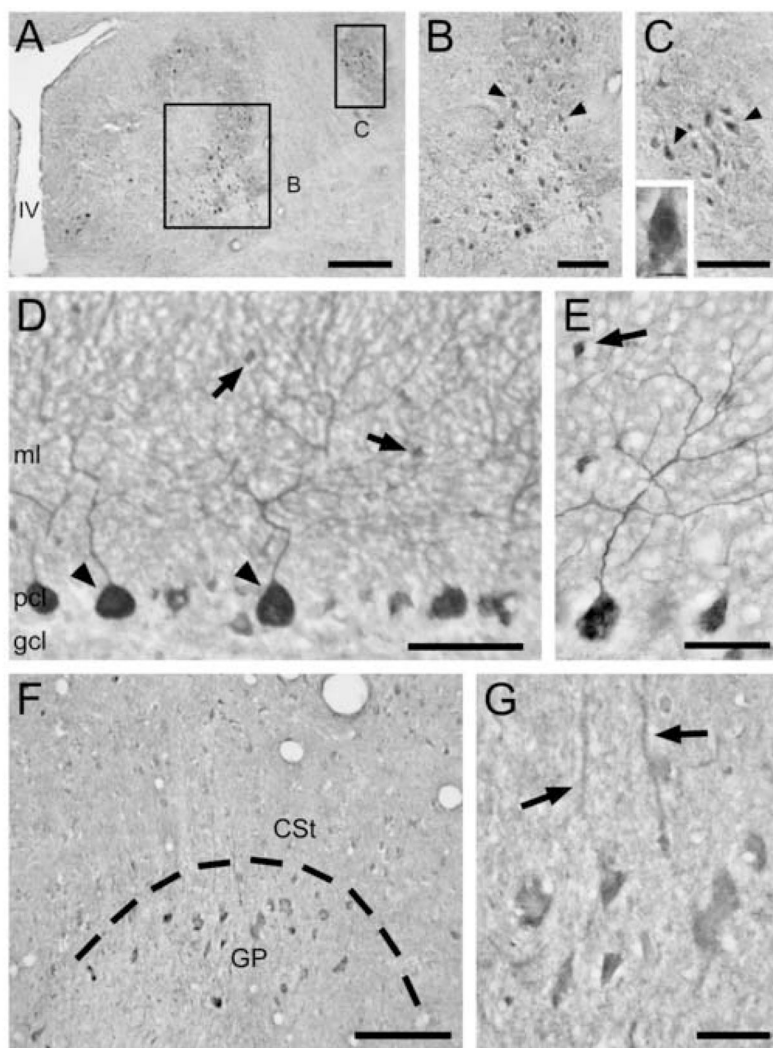


**Figure 3. GABA immunoreactivity in known GABAergic neurons in zebra finches**

(A) Low power view of a frontal section depicting strongly labeled cells in the deep cerebellar nuclei. Rectangles illustrate where photomicrographs in (B) and (C) were taken from. (B) and (C) Detailed views of middle and lateral cerebellar nuclei depicting a moderate density of strongly immunolabeled cells. Arrowheads indicate examples of cells with triangular and elongated somata. Inset in (C) shows a high power view of one labeled neuron. (D) View of part of a cerebellar folium, depicting labeling of Purkinje cells; arrowheads indicate examples of immunopositive cells with immunonegative nucleus. Arrows depict small labeled cells in the molecular layer. (E) Detail view of cerebellar Purkinje cells and respective dendritic arborizations. Arrow depicts putative basket cell in the molecular layer. (F) Low power photomicrograph of the transition between the GP and CSt. Note that GABA-positive cells are strongly labeled and highly concentrated in the dorsal aspect of the GP, but are found at very low densities in the CSt. (G) High power view of GP depicting somata of labeled cells and respective dendrites extending into the CSt (arrows). Scale bars (in  $\mu\text{m}$ ): 250 (A); 100 (B–C); 12.5 (inset C); 50 (D); 25 (E); 100 (F); 25 (G). For abbreviations, see list.

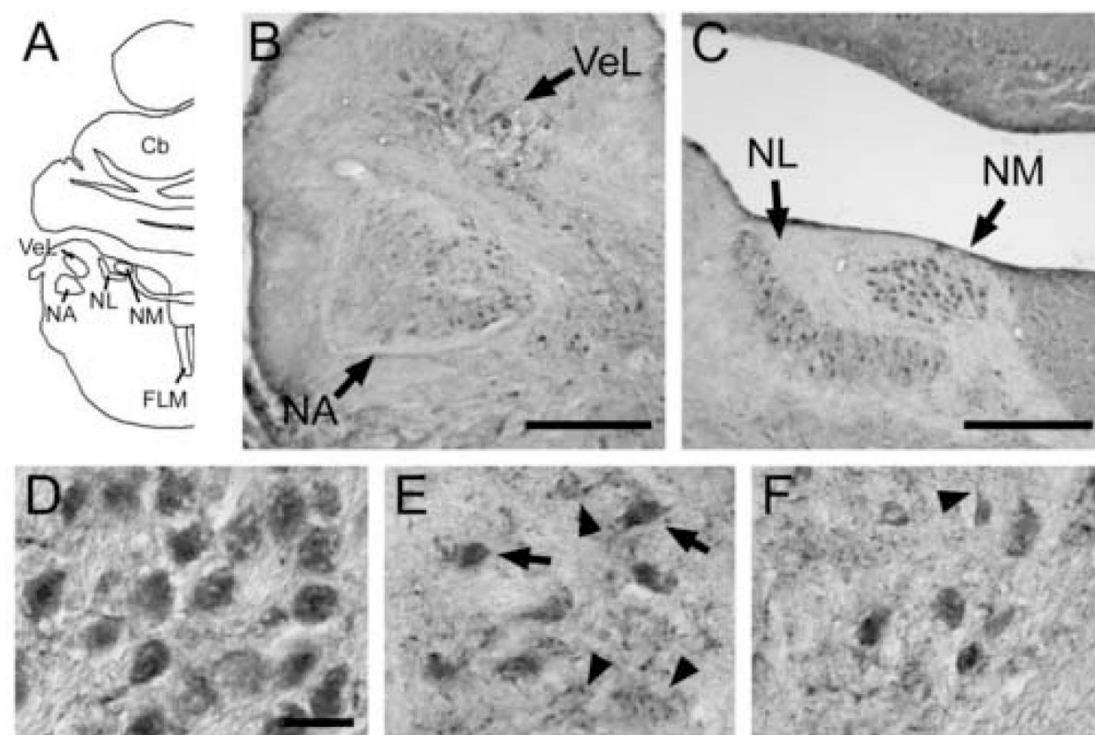


**Figure 4. GABA immunoreactivity in cochlear nuclei and nucleus laminaris**

(A) Camera lucida drawing of left half of a frontal section indicating the location of cochlear nuclei. (B) Low power photomicrograph depicting GABA immunoreactivity in NA. Note that labeled cells are more frequent medially. Prominently labeled cells can also be seen in the adjacent VeL. (C) Low power photomicrograph depicting GABA immunolabeled neurons in NM and NL. (D–F) High power photomicrographs of NM, NL and NA, respectively, depicting the pattern of GABA staining in these nuclei. Arrows in E indicate immunopositive cells, arrowheads indicate coarse punctate staining over immunonegative cells. Arrowhead in F indicates immunolabeled process extending from a GABA-positive soma. Scale bars (in  $\mu\text{m}$ ): 250 (B–C); 25 (D–F).

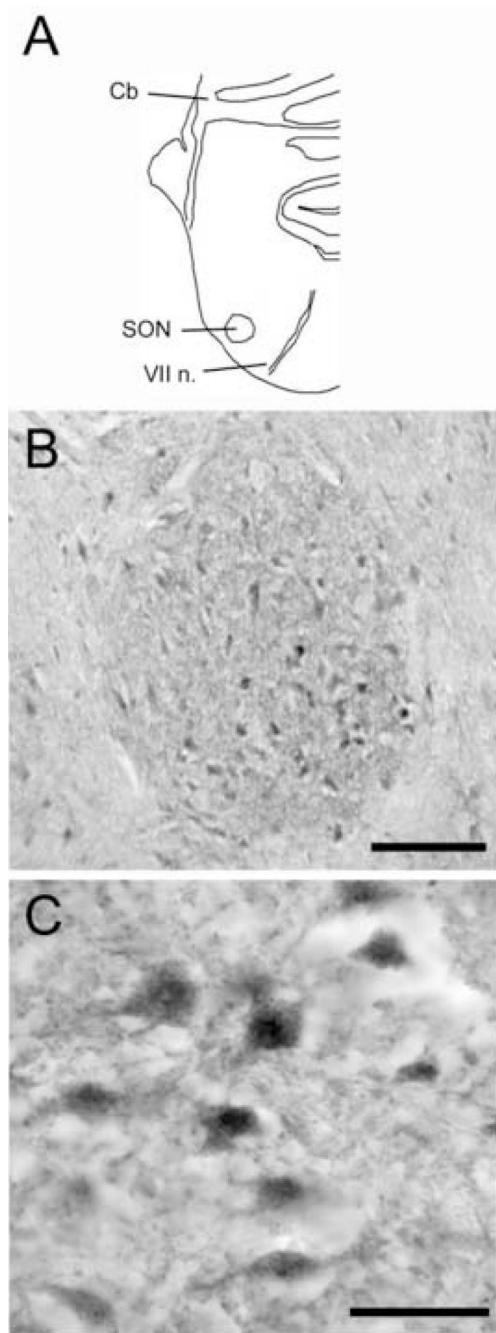


**Figure 5. GABA-positive neurons in the SON**

(A) Camera lucida drawing of frontal section at the level of the superior olivary nucleus, where photomicrographs B and C were obtained from. (B) Low power photomicrograph depicting the distribution pattern of labeled cells in the SON. Note that these cells are found at a higher density ventrally. (C) High power photomicrograph illustrating GABA-immunopositive neurons and puncta. Scale bars (in  $\mu\text{m}$ ): 100 (B); 25 (C).

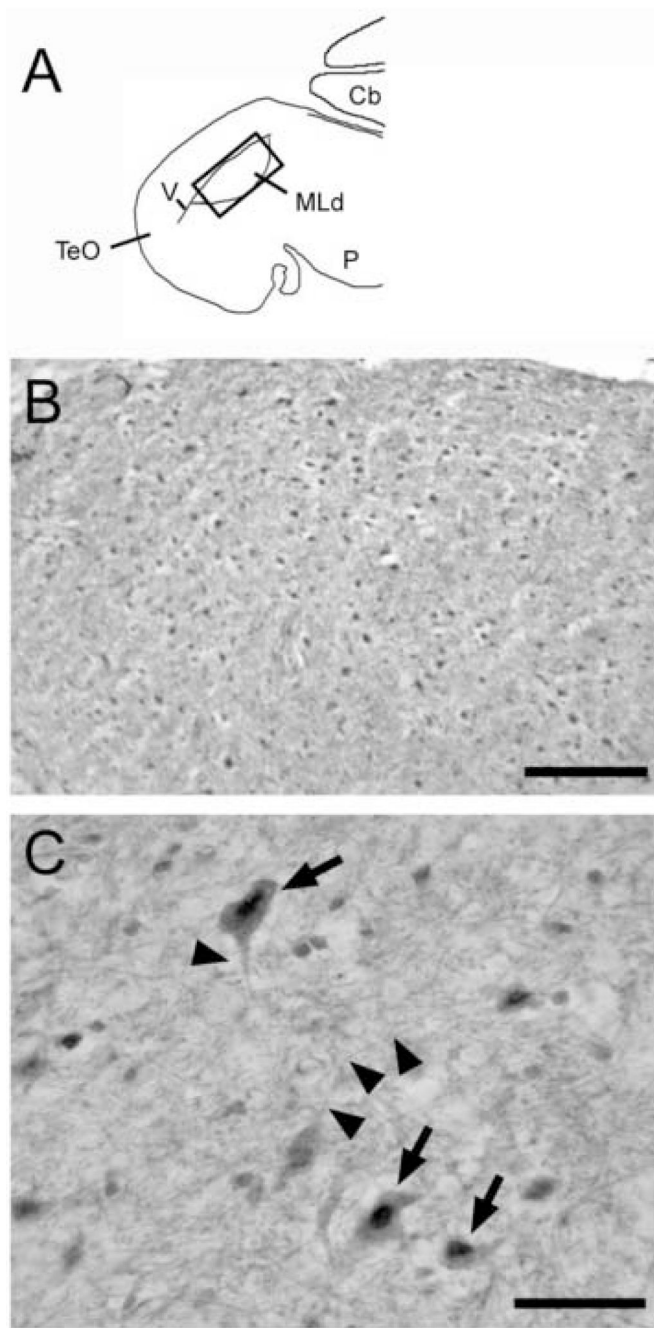


**Figure 6. GABA immunoreactivity in MLd**

(A) Camera lucida drawing of the left half of a frontal section depicting nucleus MLd and adjacent brain areas. The box represents the location where the photomicrograph in B was taken. (B) Low power photomicrograph depicting the distribution of labeled cells in MLd. (C) Detail view of labeled cells. Arrows show typical examples of cells with strong immunostaining over the nucleus and less intense cytoplasmic labeling. Arrowheads indicate processes that extend to form an intricate neuritic network. Scale bars (in  $\mu\text{m}$ ): 250 (B); 25 (C).

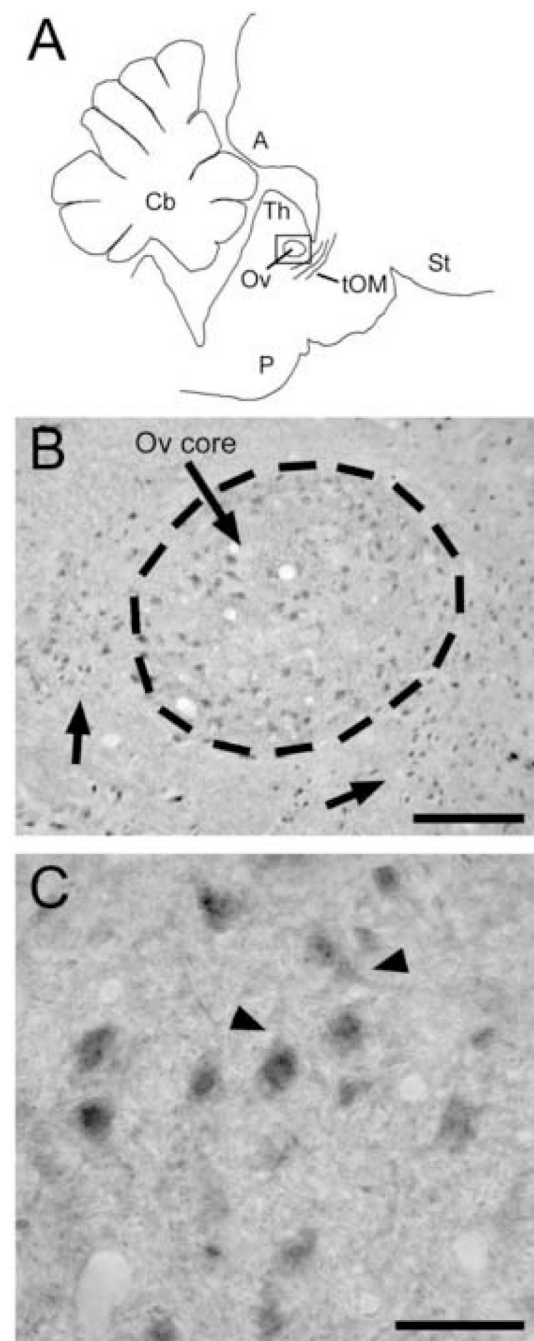


**Figure 7. GABA immunoreactivity in Ov**

(A) Camera lucida drawing of parasagittal section through nucleus Ov depicting its position relative to adjacent brain structures. The box illustrates where the photomicrograph B was taken from. (B) Low power photomicrograph illustrating the distribution of GABA-immunolabeled neurons in the core and shell (arrows) regions of Ov. (C) High power photomicrograph depicting immunolabeled cells in the Ov core. Arrowheads indicate immunolabeled processes that extended from strongly labeled cells. Scale bars (in  $\mu\text{m}$ ): 100 (B); 25 (C).

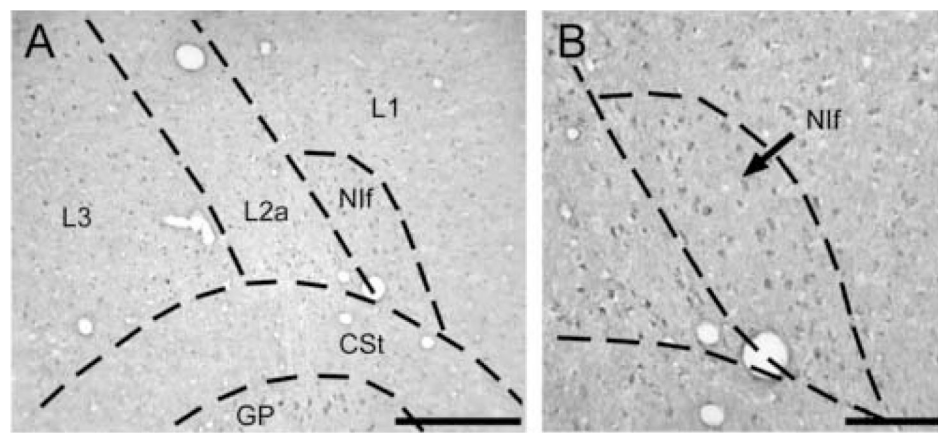


**Figure 8. GABA immunoreactivity in field L and NIIf**

(A) Low power photomicrograph depicting GABA-immunoreactivity in all field L subdivisions (L1, L2a and L3) and NIIf. Note that the ventral border of these regions can be clearly defined by the very low density of labeled cells in the CSt. (B) Photomicrograph showing detailed view of GABA-labeled cells in NIIf. Scale bars (in  $\mu\text{m}$ ): 250 (A); 100 (B).

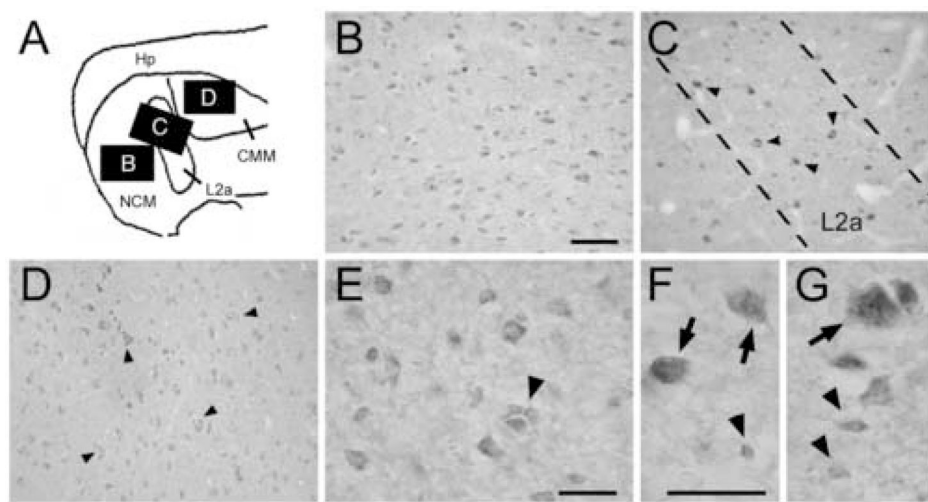


**Figure 9. GABA immunoreactivity in auditory areas of the caudomedial telencephalon**

(A) Camera lucida drawing of parasagittal section through auditory areas in the caudomedial telencephalon. Boxes indicate the locations of areas shown in panels B–D. (B–D) Low power views depicting GABA-labeled cells in (B) NCM, (C) field L2a, and (D) CMM; dashed lines indicate approximate borders of field L2a based on Nissl counterstaining of adjacent section. Arrowheads in (C) indicate some of the large labeled cells in L2a; arrowheads in (D) indicate some labeled cell clusters in CMM. (E) Detailed view depicting heterogeneity of size and shapes of GABA-labeled cells in NCM, and one labeled cell cluster (arrowhead). (F–G) High power photomicrographs depicting large (arrows) and small (arrowheads) labeled cells in NCM. Scale bars (in  $\mu\text{m}$ ): 50 (B–D); 25 (E); 50 (F–G).

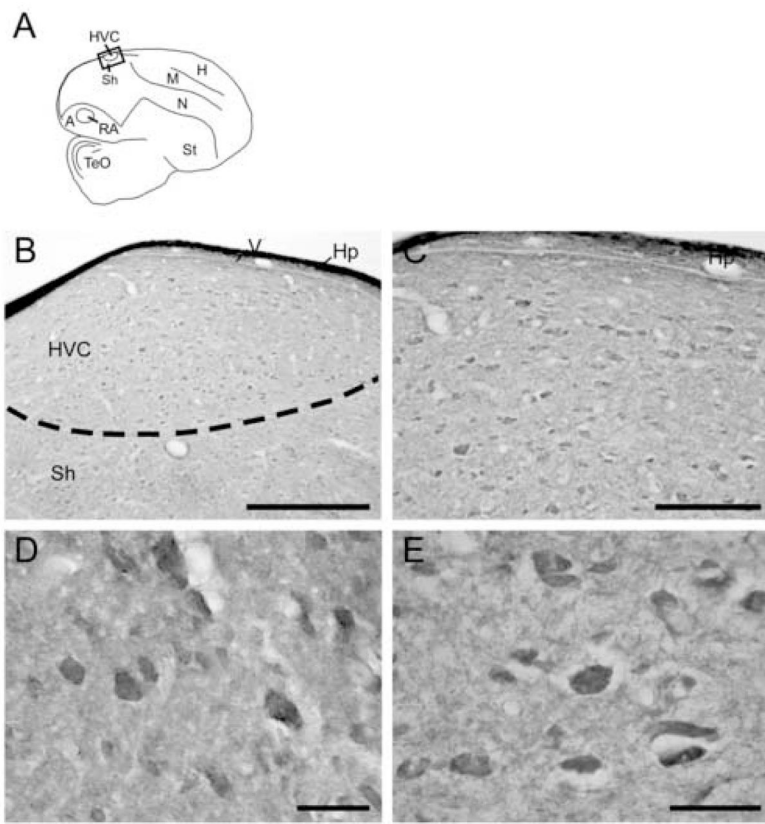


**Figure 10. GABA immunoreactivity in HVC and the nidopallial shelf area**

(A) Camera lucida drawing of parasagittal section depicting the location of song nucleus HVC and the adjacent shelf area. Box shows the area where photomicrograph in B was taken. (B) Low power photomicrograph depicting the distribution of labeled cells in HVC and the shelf area. (C) View of the distribution of GABA-labeled cells in HVC. (D–E) High power photomicrographs depicting labeled cells in the shelf area and HVC, respectively, detailing the morphology and staining patterns of these cells. Scale bars (in  $\mu\text{m}$ ): 250 (B); 100 (C); 25 (D–E).

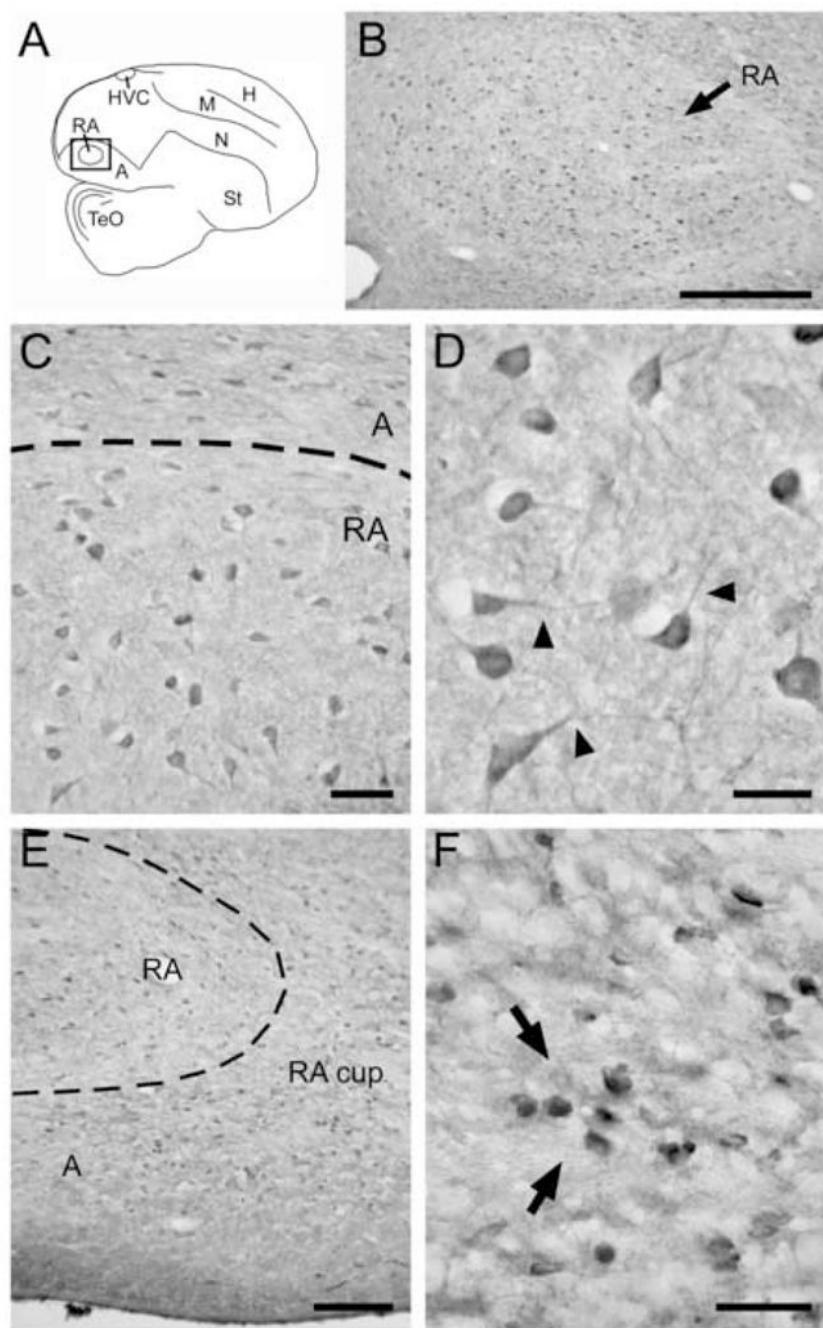


**Figure 11. GABA immunoreactivity in RA and the arcopallial cup area**

(A) Camera lucida drawing of parasagittal section illustrating the relative position of song nucleus RA and adjacent structures. The box indicates where the picture in B was taken. (B) Low power photomicrograph illustrating the general distribution of labeled cells in nucleus RA. Note the lower density of labeled cells in the surrounding tissue. (C) Detail view of labeled cells in RA and adjacent arcopallium. Dashed line indicates the boundary of RA based on Nissl counterstaining. (D) High power photomicrograph of GABA-labeled cells within RA. Arrowheads indicate immunolabeled processes that extend from labeled cells, branch, and form an intricate fiber network. (E) Low power photomicrograph depicting GABA-positive cells in the cup region, adjacent to RA. Dashed line indicates the rostral boundary of RA, as defined

by Nissl counterstaining. (F) High power photomicrograph depicting uneven distribution of GABAergic cells in the cup region. Arrows indicate example of a loose group of cells. Scale bars (in  $\mu\text{m}$ ): 250 (B); 50 (C); 25 (D); 100 (E); 25 (F).

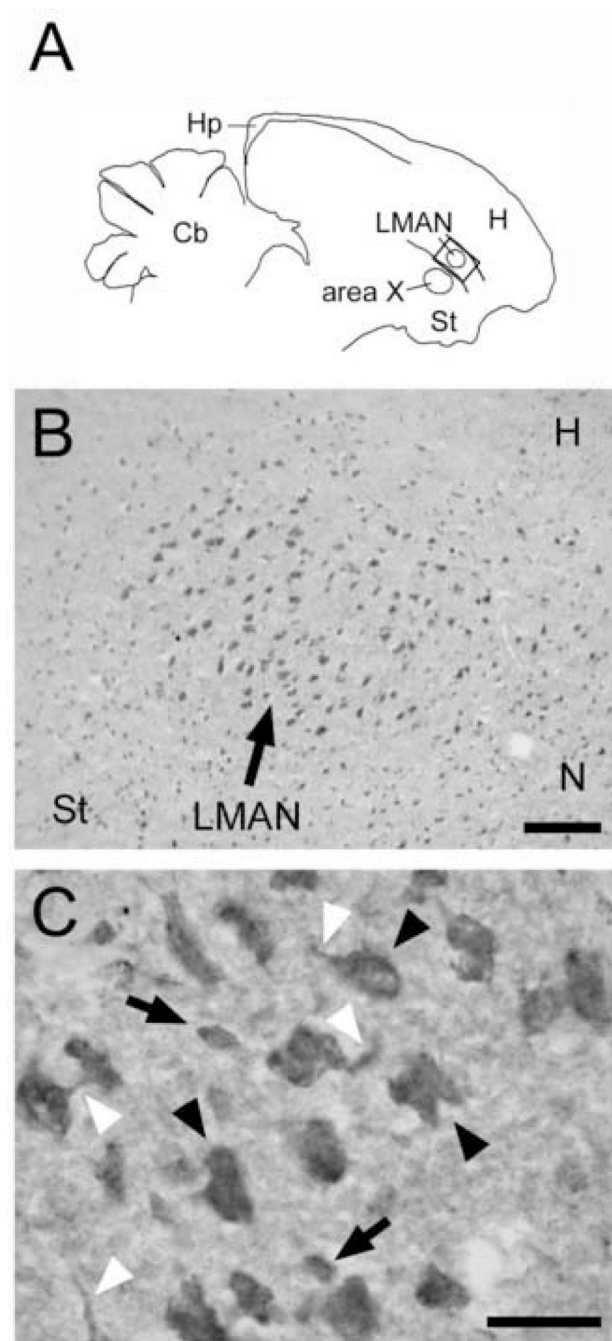


**Figure 12. GABA immunoreactivity in LMAN**

(A) Camera lucida drawing of parasagittal section indicating the relative position of LMAN and adjacent structures. The box indicates the location where the picture in B was taken. (B) Low power photomicrograph depicting the distribution of labeled cells in LMAN. Note the marked difference in cell size and labeling in LMAN compared to adjacent regions. (C) High power photomicrograph of labeled cells in LMAN. Large cells (black arrowheads) were more abundant and varied in shape than small cells (arrows). Immunolabeled processes (white arrowheads) were primarily associated with larger neurons. Scale bars (in  $\mu\text{m}$ ): 100 (B); 25 (C).

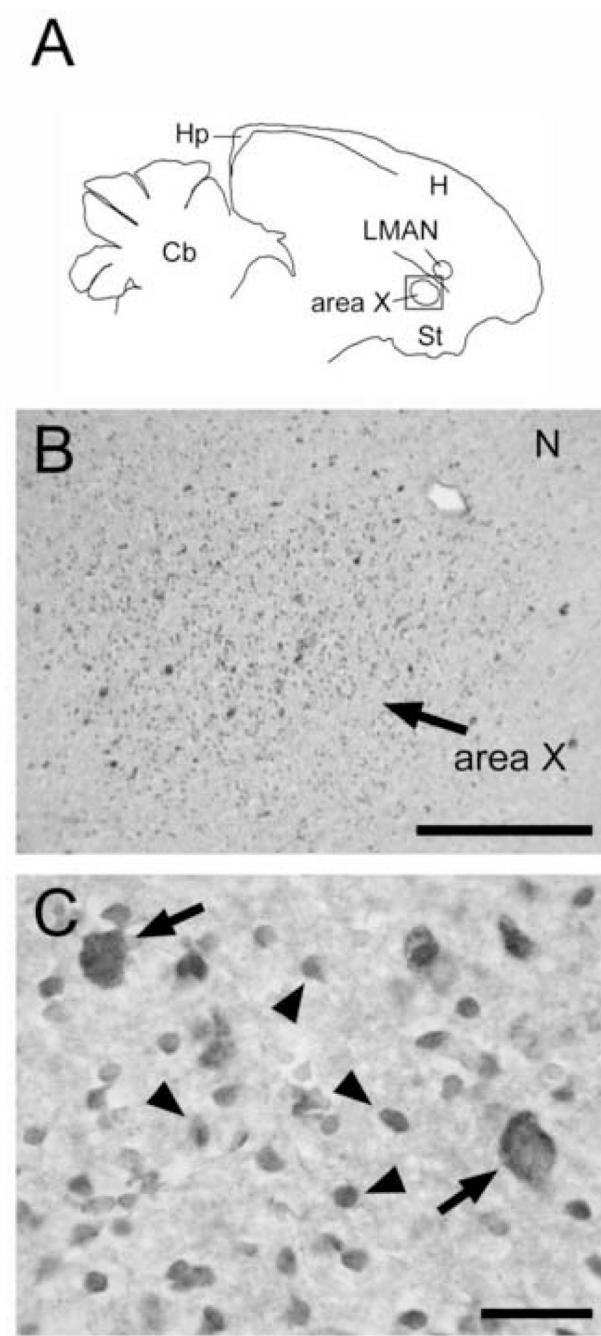


**Figure 13. GABA immunoreactivity in area X**

(A) Camera lucida drawing of parasagittal section illustrating the position of area X and adjacent brain areas. (B) Low power photomicrograph depicting the overall distribution of GABAergic neurons in area X. Note the higher density of GABAergic cells compared to the adjacent regions. (C) High power photomicrograph depicting the smaller (arrowheads) and larger (arrows) GABAergic cells in area X. Both types were evenly distributed throughout this nucleus. Scale bars (in  $\mu\text{m}$ ): 250 (B); 25 (C).

**TABLE 1**

Structure	Average Cell Diameter ( $\mu\text{m} \pm \text{S.E.}$ )	Range of Cell Diameters ( $\mu\text{m}$ )
NA	$11.1 \pm 0.6$	5.6–15.8
NL	$9.7 \pm 0.3$	5.7–13.7
NM	$18.2 \pm 0.5$	12.2–26.4
SON	$7.6 \pm 0.3$	3.9–12.4
MLd	$16.0 \pm 0.9$	6.7–28.4
Ov	$6.7 \pm 0.2$	3.7–9.2
L1	$9.4 \pm 0.3$	4.1–15.1
L2a	$13.2 \pm 0.4$	5.2–21.8
L3	$10.8 \pm 0.4$	4.9–18.6
NCM	$9.2 \pm 0.6$	3.3–20.8
CMM	$7.0 \pm 0.5$	3.9–19.3
Shelf	$8.9 \pm 0.5$	3.4–16.0
Cup	$7.1 \pm 0.2$	4.4–10.5
NI $\ddagger$	$9.4 \pm 0.5$	3.4–16.7
HVC	$10.7 \pm 0.4$	6.7–14.3
RA	$14.3 \pm 0.7$	6.4–28.5
LMAN	$12.5 \pm 0.5$	5.0–23.8
Area X	$7.1 \pm 0.5$	3.6–22.6

\* Auditory structures are listed according to position along the ascending pathway, followed by song control nuclei.